# A general power equation for predicting bed load transport rates in gravel bed rivers

Jeffrey J. Barry

Department of Civil Engineering, Ecohydraulics Research Group, University of Idaho, Boise, Idaho, USA

Boise Cascade Corporation, Timberland Resources, Boise, Idaho, USA

John M. Buffington and John G. King

Rocky Mountain Research Station, Forest Service, U.S. Department of Agriculture, Boise, Idaho, USA

Received 16 March 2004; revised 23 July 2004; accepted 18 August 2004; published 27 October 2004.

[1] A variety of formulae has been developed to predict bed load transport in gravel bed rivers, ranging from simple regressions to complex multiparameter formulations. The ability to test these formulae across numerous field sites has, until recently, been hampered by a paucity of bed load transport data for gravel bed rivers. We use 2104 bed load transport observations in 24 gravel bed rivers in Idaho to assess the performance of eight different formulations of four bed load transport equations. Results show substantial differences in performance but no consistent relationship between formula performance and degree of calibration or complexity. However, formulae containing a transport threshold typically exhibit poor performance. Furthermore, we find that the transport data are best described by a simple power function of discharge. From this we propose a new bed load transport equation and identify channel and watershed characteristics that control the exponent and coefficient of the proposed power function. We find that the exponent is principally a factor of supply-related channel armoring (transport capacity in excess of sediment supply), whereas the coefficient is related to drainage area (a surrogate for absolute sediment supply). We evaluate the accuracy of the proposed power function at 17 independent test sites. *INDEX TERMS:* 1824 Hydrology: Geomorphology (1625); 1815 Hydrology: Erosion and sedimentation; 3210 Mathematical Geophysics: Modeling; *KEYWORDS:* gravel bed rivers, sediment transport, fluvial geomorphology

**Citation:** Barry, J. J., J. M. Buffington, and J. G. King (2004), A general power equation for predicting bed load transport rates in gravel bed rivers, *Water Resour. Res.*, *40*, W10401, doi:10.1029/2004WR003190.

## 1. Introduction

[2] *Fang* [1998] remarked on the need for a critical evaluation and comparison of the plethora of sediment transport formulae currently available. In response, *Yang and Huang* [2001] evaluated the performance of 13 sediment transport formulae in terms of their ability to describe the observed sediment transport from 39 data sets (a total of 3391 transport observations). They concluded that sediment transport formulae based on energy dissipation rates or stream power concepts more accurately described the observed transport data and that the degree of formula complexity did not necessarily translate into increased model accuracy. Although the work of *Yang and Huang* [2001] is helpful in evaluating the applicability and accuracy of many popular sediment transport equations, it is necessary to extend their analysis to coarse-grained natural rivers. Of the 39 data sets used by *Yang and Huang* [2001], only 5 included observations from natural channels (166 transport observations) and these were limited to sites with a fairly uniform grain-size distribution (gradation coefficient $\leq 2$).

Copyright 2004 by the American Geophysical Union.
0043-1397/04/2004WR003190$09.00

[3] Prior to the extensive work of *Yang and Huang* [2001], *Gomez and Church* [1989] performed a similar analysis of 12 bed load transport formulae using 88 bed load transport observations from 4 natural gravel bed rivers and 45 bed load transport observations from 3 flumes. The authors concluded that none of the selected formulae performed consistently well, but they did find that formula calibration increases prediction accuracy. However, similar to *Yang and Huang* [2001], *Gomez and Church* [1989] had limited transport observations from natural gravel bed rivers.

[4] *Reid et al.* [1996] assessed the performance of several popular bed load formulae in the Negev Desert, Israel, and found that the *Meyer-Peter and Müller* [1948] and *Parker* [1990] equations performed best, but their analysis considered only one gravel bed river. Because of small sample sizes, these prior investigations leave the question unresolved as to the performance of bed load transport formulae in coarse-grained natural channels.

[5] Recent work by *Martin* [2003], *Bravo-Espinosa et al.* [2003] and *Almedeij and Diplas* [2003] has begun to address this deficiency. *Martin* [2003] took advantage of 10 years of sediment transport and morphologic surveys on the Vedder River, British Columbia, to test the performance of the *Meyer-Peter and Müller* [1948] equation and two

variants of the *Bagnold* [1980] equation. The author concluded that the formulae generally underpredict gravel transport rates and suggested that this may be due to loosened bed structure or other disequilibria resulting from channel alterations associated with dredge mining within the watershed.

[6] *Bravo-Espinosa et al.* [2003] considered the performance of seven bed load transport formulae on 22 alluvial streams (including a subset of the data examined here) in relation to a site-specific "transport category" (i.e., transport limited, partially transport limited and supply limited). The authors found that certain formulae perform better under certain categories of transport and that, overall, the *Schoklitsch* [1950] equation performed well at eight of the 22 sites, while the *Bagnold* [1980] equation performed well at seven of the 22 sites.

[7] *Almedeij and Diplas* [2003] considered the performance of the *Meyer-Peter and Müller* [1948], H. A. Einstein and C. B. Brown (as discussed by *Brown* [1950]), *Parker* [1979], and *Parker et al.* [1982] bed load transport equations on three natural gravel bed streams, using a total of 174 transport observations. The authors found that formula performance varied between sites, in some cases overpredicting observed bed load transport rates by one to three orders of magnitude, while at others underpredicting by up to two orders of magnitude.

[8] Continuing these recent studies of bed load transport in gravel bed rivers, we examine 2104 bed load transport observations from 24 study sites in mountain basins of Idaho to assess the performance of four bed load transport equations. We also assess accuracy in relation to the degree of formula calibration and complexity.

[9] Unlike *Gomez and Church* [1989] and *Yang and Huang* [2001], we find no consistent relationship between formula performance and the degree of formula calibration and complexity. However, like *Whiting et al.* [1999], we find that the observed transport data are best fit by a simple power function of total discharge. We propose this power function as a new bed load transport equation and explore channel and watershed characteristics that control the exponent and coefficient of the observed bed load power functions. We hypothesize that the exponent is principally a function of supply-related channel armoring, such that mobilization of the surface material in a well armored channel is followed by a relatively larger increase in bed load transport rate (i.e., steeper rating curve) than that of a similar channel with less surface armoring [*Emmett and Wolman*, 2001]. We use *Dietrich et al.*'s [1989] dimensionless bed load transport ratio ($q^*$) to quantify channel armoring in terms of upstream sediment supply relative to transport capacity, and relate $q^*$ values to the exponents of the observed bed load transport functions. We hypothesize that the power function coefficient depends on absolute sediment supply, which we parameterize in terms of drainage area.

[10] The purpose of this paper is fourfold: (1) assess the performance of four bed load transport formulae in mountain gravel bed rivers, (2) use channel and watershed characteristics to parameterize the coefficient and exponent of our bed load power function to make it a predictive equation, (3) test the parameterization equations, and (4) compare the performance of our proposed bed load transport function to that of the other equations in item 1.

## 2. Bed Load Transport Formulae

[11] We compare predicted total bed load transport rates to observed values at each study site using four common transport equations, and we examine how differences in formula complexity and calibration influence performance. In each equation we use the characteristic grain size as originally specified by the author(s) to avoid introducing error or bias. We also examine several alternative definitions to investigate the effects of grain size calibration on formula performance. Variants of other parameters in the bed load equations are not examined, but could also influence performance.

[12] Eight variants of four formulae were considered: the *Meyer-Peter and Müller* [1948] equation (calculated both by median subsurface grain size, $d_{50ss}$, and by size class, $d_i$), the *Ackers and White* [1973] equation as modified by *Day* [1980] (calculated by $d_i$), the *Bagnold* [1980] equation (calculated by the modal grain size of each bed load event, $d_{mqb}$, and by the mode of the subsurface material, $d_{mss}$), and the *Parker et al.* [1982] equation as revised by *Parker* [1990] (calculated by $d_{50ss}$ and two variants of $d_i$). We use the subsurface-based version of the *Parker* [1990] equation because the surface-based one requires site-specific knowledge of how the surface size distribution evolves with discharge and bed load transport (information that was not available to us and that we did not feel confident predicting). The formulae are further described in Appendix A and are written in terms of specific bed load transport rate, defined as dry mass per unit width and time ($q_b$, kg m$^{-1}$ s$^{-1}$).

[13] Two variants of the size-specific ($d_i$) *Parker et al.* [1982] equation are considered, one using a site-specific hiding function following *Parker et al.*'s [1982] method and the other using *Andrews*' [1983] hiding function. These two variants allow comparison of site-specific calibration versus use of an "off-the-shelf" hiding function for cases where bed load transport data are not available. We selected the *Andrews* [1983] hiding function because it was derived from channel types and physiographic environments similar to those examined in this study. We also use single grain size ($d_{50ss}$) and size-specific ($d_i$) variants of the *Meyer-Peter and Müller* [1948] and *Parker et al.* [1982] equations to further examine effects of grain size calibration. In this case, we compare predictions based on a single grain size ($d_{50ss}$) versus those summed over the full range of size classes available for transport ($d_i$). We also consider two variants of the *Bagnold* [1980] equation, one where the representative grain size is defined as the mode of the observed bed load data ($d_{mqb}$, as specified by *Bagnold* [1980]) and one based on the mode of the subsurface material ($d_{mss}$, an approach that might be used where bed load transport observations are unavailable). The latter variant of the *Bagnold* [1980] equation is expected to be less accurate because it uses a static grain size (the subsurface mode), rather than the discharge-specific mode of the bed load.

[14] The transport equations were solved for flow and channel conditions present during bed load measurements and are calibrated to differing degrees to site-specific

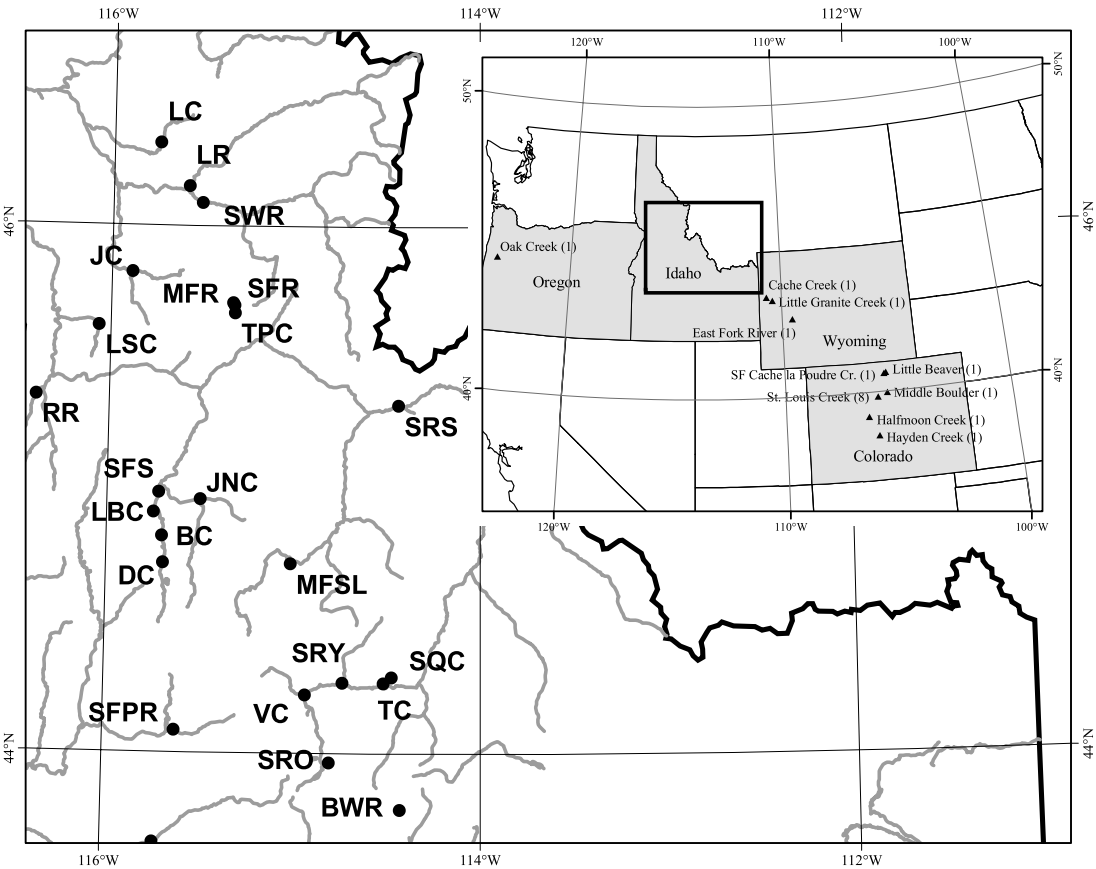


**Figure 1.** Location of bed load transport study sites. Table 1 lists river names abbreviated here. Inset box shows the location of test sites outside of Idaho. Parentheses next to test site names indicate number of data sets at each site.

conditions. For example, the *Meyer-Peter and Müller* [1948] formula includes a shear stress correction based on the ratio of particle roughness to total roughness, where particle roughness is determined from surface grain size and the *Strickler* [1923] equation, and total roughness is determined from the *Manning* [1891] equation for observed values of hydraulic radius and water-surface slope (Appendix A).

[15] Except for the *Parker et al.* [1982] equation, each of the formulae used in our analysis are similar in that they contain a threshold for initiating bed load transport. The *Meyer-Peter and Müller* [1948] equation is a power function of the difference between applied and critical shear stresses, the *Ackers and White* [1973] equation is a power function of the ratio of applied to critical shear stress minus 1, and the *Bagnold* [1980] equation is a power function of the difference between applied and critical unit stream power (Appendix A). In contrast, the *Parker et al.* [1982] equation lacks a transport threshold and predicts some degree of transport at all discharges, similar to *Einstein*'s [1950] equation.

## 3. Study Sites and Methods

[16] Data obtained by *King et al.* [2004] from 24 mountain gravel bed rivers in central Idaho were used to assess the performance of different bed load transport equations and to develop our proposed power function for bed load transport (Figure 1). The 24 study sites are single-thread channels with pool-riffle or plane-bed morphology (as defined by *Montgomery and Buffington* [1997]). Banks are typically composed of sand, gravel and cobbles with occasional boulders, are densely vegetated and appear stable. An additional 17 study sites in Oregon, Wyoming and Colorado were used to test our new bed load transport equation (Figure 1). Selected site characteristics are given in Table 1.

[17] *Whiting and King* [2003] describes the field methods at 11 of our 24 Idaho sites (also see *Moog and Whiting* [1998], *Whiting et al.* [1999] and *King et al.* [2004] for further information on the sites). Bed load samples were obtained using a 3-inch Helley-Smith [*Helley and Smith*, 1971] sampler, which limits the sampled bed load material to particle sizes less than about 76 mm. Multiple lines of evidence, including movement of painted rocks and bed load captured in large basket samplers at a number of the 24 Idaho sites, indicate that during the largest flows almost all sizes found on the streambed are mobilized, including sizes larger than the orifice of the Helley-Smith sampler. However, transport-weighted composite samples across all study sites indicate that only a very small percentage of the observed particles in motion approached the size limit of the Helley-Smith sampler. Therefore, although larger particles are in motion during flood flows, the motion of these particles is infrequent and the likelihood of sampling these larger particles is small.

[18] Each bed load observation is a composite of all sediment collected over a 30 to 60 second sample period,

**Table 1.** Study and Test Site Characteristics

| Site (Abbreviation) | Drainage Area, $km^2$ | Average Slope, $m\ m^{-1}$ | Subsurface $d_{50ss}$, mm | Surface $d_{50s}$, mm | 2-Year Flood, $m^3\ s^{-1}$ |
|---|---|---|---|---|---|
| | | *Study Sites* | | | |
| Little Buckhorn Creek (LBC) | 16 | 0.0509 | 15 | 74 | 2.79 |
| Trapper Creek (TPC) | 21 | 0.0414 | 17 | 75 | 2.21 |
| Dollar Creek (DC) | 43 | 0.0146 | 22 | 83 | 11.8 |
| Blackmare Creek (BC) | 46 | 0.0299 | 25 | 101 | 6.95 |
| Thompson Creek (TC) | 56 | 0.0153 | 44 | 62 | 3.10 |
| SF Red River (SFR) | 99 | 0.0146 | 25 | 95 | 8.7 |
| Lolo Creek (LC) | 106 | 0.0097 | 19 | 85 | 16.9 |
| MF Red River (MFR) | 129 | 0.0059 | 18 | 57 | 12.8 |
| Little Slate Creek (LSC) | 162 | 0.0268 | 24 | 134 | 16.0 |
| Squaw Creek (SQC) | 185 | 0.0100 | 29 | 46 | 6.62 |
| Salmon River near Obsidian (SRO) | 243 | 0.0066 | 26 | 61 | 14.8 |
| Rapid River (RR) | 280 | 0.0108 | 16 | 75 | 20.3 |
| Johns Creek (JC) | 293 | 0.0207 | 36 | 204 | 36.8 |
| Big Wood River (BWR) | 356 | 0.0091 | 25 | 119 | 26.2 |
| Valley Creek (VC) | 386 | 0.0040 | 21 | 50 | 28.3 |
| Johnson Creek (JNC) | 560 | 0.0040 | 14 | 62 | 83.3 |
| SF Salmon River (SFS) | 853 | 0.0025 | 14 | 38 | 96.3 |
| SF Payette River (SFPR) | 1164 | 0.0040 | 20 | 95 | 120 |
| Salmon River below Yankee Fork (SRY) | 2101 | 0.0034 | 25 | 104 | 142 |
| Boise River (BR) | 2154 | 0.0038 | 21 | 60 | 188 |
| MF Salmon River at Lodge (MFSL) | 2694 | 0.0041 | 36 | 146 | 258 |
| Lochsa River (LR) | 3055 | 0.0023 | 27 | 132 | 532 |
| Selway River (SWR) | 4955 | 0.0021 | 24 | 185 | 731 |
| Salmon River at Shoup (SRS) | 16154 | 0.0019 | 28 | 96 | 385 |
| | | *Test Sites* | | | |
| Fool Creek (St. Louis Creek Test Site) | 3 | 0.0440 | 15 | 38 | 0.320 |
| Oak Creek | 7 | 0.0095 | 20 | 53 | 2.98 |
| East St. Louis Creek | 8 | 0.0500 | 13 | 51 | 0.945 |
| St. Louis Creek Site 5 | 21 | 0.0480 | 14 | 146 | 2.52 |
| Cache Creek | 28 | 0.0210 | 20 | 46 | 2.2 |
| St. Louis Creek Site 4a | 34 | 0.0190 | 13 | 72 | 3.96 |
| St. Louis Creek Site 4 | 34 | 0.0190 | 13 | 91 | 3.99 |
| Little Beaver Creek | 34 | 0.2300 | 10 | 47 | 2.24 |
| Hayden Creek | 47 | 0.0250 | 20 | 68 | 2.28 |
| St. Louis Creek Site 3 | 54 | 0.0160 | 16 | 82 | 5.07 |
| St. Louis Creek Site 2 | 54 | 0.0170 | 15 | 76 | 5.08 |
| Little Granite Creek | 55 | 0.0190 | 18 | 55 | 8.41 |
| St. Louis Creek Site 1 | 56 | 0.0390 | 17 | 129 | 5.21 |
| Halfmoon Creek | 61 | 0.0150 | 18 | 62 | 7.3 |
| Middle Boulder Creek | 83 | 0.0128 | 25 | 75 | 12.6 |
| SF Cache la Poudre | 231 | 0.0070 | 12 | 69 | 13.8 |
| East Fork River | 466 | 0.0007 | 1 | 5 | 36.0 |

depending on flow conditions, at typically 20 equally spaced positions across the width of the wetted channel [*Edwards and Glysson*, 1999]. Between 43 and 192 nonzero bed load transport measurements were collected over a 1 to 7 year period and over a range of discharges from low flows to those well in excess of the bank-full flood at each of the 24 Idaho sites.

[19] Channel geometry and water surface profiles were surveyed following standard field procedures [*Williams et al.*, 1988]. Surveyed reaches were typically 20 channel widths in length. At eight sites water surface slopes were measured over a range of discharges and did not vary significantly. Hydraulic geometry relations for channel width, average depth and flow velocity were determined from repeat measurements over a wide range of discharges.

[20] Surface and subsurface particle size distributions were measured at a minimum of three locations at each of the study sites during low flows between 1994 and 2000. Where surface textures were fairly uniform throughout the study reach, three locations were systematically selected for sampling surface and subsurface material. If major textural differences were observed, two sample sites were located within each textural patch, and measurements were weighted by patch area [e.g., *Buffington and Montgomery*, 1999a]. *Wolman* [1954] pebble counts of $100^+$ surface grains were conducted at each sample site. Subsurface samples were obtained after removing the surface material to a depth equal to the $d_{90}$ of surface grains and were sieved by weight. The *Church et al.* [1987] sampling criterion was generally met, such that the largest particle in the sample comprised, on average, about 5% of the total sample weight. However, at three sites (Johns Creek, Big Wood River and Middle Fork Salmon River) the largest particle comprised 13%–14% of the total sample weight; the Middle Fork Salmon River is later excluded for other reasons.

[21] Estimates of flood frequency were calculated using a log Pearson III analysis [*U.S. Water Resources Council*, 1981] at all study sites that had at least a 10 year record of instantaneous stream flow. Only five years of flow data were available at Dollar and Blackmare creeks, and therefore estimates of flood frequency were calculated using a two-station comparison [*U.S. Water Resources Council*,

1981] based on nearby, long-term USGS stream gages. A regional relationship between drainage area and flood frequency was used at Little Buckhorn Creek due to a lack instantaneous peak flow data.

[22] Each sediment transport observation at the 24 Idaho sites was reviewed for quality. At nine of the sites all observations were included. Of the remaining 15 sites, a total of 284 transport observations (out of 2388) were removed (between 2 and 51 observations per site). The primary reasons for removal were differences in sampling method prior to 1994, or because the transport observations were taken at a different, or unknown, location compared to the majority of bed load transport samples. Only 41 transport observations (out of 284) from nine sites were removed due to concerns regarding sample quality (i.e., significant amounts of measured transport at extremely low discharges indicative of "scooping" during field sampling).

[23] Methods of data collection varied greatly among the additional 17 test sites outside of Idaho and are described in detail elsewhere (see *Ryan and Emmett* [2002] for Little Granite Creek, Wyoming; *Leopold and Emmett* [1997] for the East Fork River, Wyoming; *Milhous* [1973] for Oak Creek, Oregon; *Ryan et al.* [2002] for the eight sites on the St. Louis River, Colorado; and *Gordon* [1995] for both Little Beaver and Middle Boulder creeks, Colorado). Data collection methods at Halfmoon Creek, Hayden Creek and South Fork Cache la Poudre Creek, Colorado and Cache Creek, Wyoming were similar to the 8 test sites from St. Louis Creek. Both the East Fork River and Oak Creek sites used channel-spanning slot traps to catch the entire bed load, while the remaining 15 test sites used a 3-inch Helley-Smith bed load sampler spanning multiple years (typically 1 to 5 years, with a maximum of 14 years at Little Granite Creek). Estimates of flood frequency were determined using either standard flood frequency analyses [*U.S. Water Resources Council*, 1981] or from drainage area–discharge relationships derived from nearby stream gages.

## 4. Results and Discussion

### 4.1. Performance of the Bed Load Transport Formulae

#### 4.1.1. Log-Log Plots

[24] Predicted total bed load transport rates for each formula were compared to observed values, with a $\log_{10}$ transformation applied to both. A logarithmic transformation is commonly applied in bed load studies because transport rates typically span a large range of values ($6^+$ orders of magnitude on a $\log_{10}$ scale), and the data tend to be skewed toward small transport rates without this transformation. To provide more rigorous support for the transformation we used the ARC program [*Cook and Weisberg*, 1999] to find the optimal Box-Cox transformation [*Neter et al.*, 1974] (i.e., one that produces a near-normal distribution of the data). Results indicate that a $\log_{10}$ transformation is appropriate, and conforms with the traditional approach for analyzing bed load transport data.

[25] Figure 2 provides an example of observed versus predicted transport rates from the Rapid River study site and indicates that some formulae produced fairly accurate, but biased, predictions of total transport. That is, predicted values were generally tightly clustered and subparallel to the 1:1 line of perfect agreement, but were typically larger than the observed values (e.g., Figure 2c). Other formulae exhibited either curvilinear bias (e.g., Figures 2b, 2f, and 2g) or rotational bias (constantly trending departure from accuracy) (e.g., Figures 2a, 2d, 2e, and 2h). On the basis of visual inspection of similar plots from all 24 sites, the *Parker et al.* [1982] equations ($d_i$ and $d_{50ss}$) best describe the observed transport rates, typically within an order of magnitude of the observed values. In contrast, the *Parker et al.* [1982] ($d_i$ via *Andrews* [1983]), *Meyer-Peter and Müller* [1948] ($d_i$ and $d_{50ss}$), and *Bagnold* [1980] ($d_{mss}$ and $d_{mqb}$) equations did not perform as well, usually over two orders of magnitude from the observed values. The *Ackers and White* [1973] equation was typically one to three orders of magnitude from the observed values.

#### 4.1.2. Transport Thresholds

[26] The above assessment of performance can be misleading for those formulae that contain a transport threshold (i.e., the *Meyer-Peter and Müller* [1948], *Ackers and White* [1973], and *Bagnold* [1980] equations). Formulae of this sort often erroneously predict zero transport at low to moderate flows that are below the predicted threshold for transport. These incorrect zero-transport predictions cannot be shown in the log-log plots of observed versus predicted transport rates (Figure 2). However, frequency distributions of the erroneous zero-transport predictions reveal substantial error for both variants of the *Meyer-Peter and Müller* [1948] equation and the *Bagnold* [1980] ($d_{mss}$) equation (Figure 3). These formulae incorrectly predict zero transport for about 50% of all observations at our study sites. In contrast, the *Bagnold* [1980] ($d_{mqb}$) and *Ackers and White* [1973] equations incorrectly predict zero transport for only 2% and 4% of the observations, respectively, at only one of the 24 study sites. Formulae that lack transport thresholds (i.e., the *Parker et al.* [1982] equation) do not predict zero transport rates.

[27] The significance of the erroneous zero-transport predictions depends on the magnitude of the threshold discharge and the portion of the total bed load that is excluded by the prediction threshold. To examine this issue we calculated the maximum discharge at which each threshold-based transport formula predicted zero transport ($Q_{\max}$) normalized by the 2-year flood discharge ($Q_2$). Many authors report that significant bed load movement begins at discharges that are 60% to 100% of bank-full flow [*Leopold et al.*, 1964; *Carling*, 1988; *Andrews and Nankervis*, 1995; *Ryan and Emmett*, 2002; *Ryan et al.*, 2002]. Bank-full discharge at the Idaho sites has a recurrence interval of 1–4.8 years, with an average of 2 years [*Whiting et al.*, 1999]; hence $Q_2$ is a bank-full-like flow. We use $Q_2$ rather than the bank-full discharge because it can be determined objectively

**Figure 2.** Comparison of measured versus computed total bed load transport rates for Rapid River (typical of the Idaho study sites): (a) *Meyer-Peter and Müller* [1948] equation by $d_{50ss}$, (b) Meyer-Peter and Müller equation by $d_i$, (c) *Ackers and White* [1973] equation by $d_i$, (d) Bagnold equation by $d_{mss}$, (e) Bagnold equation by $d_{mqb}$, (f) *Parker et al.* [1982] equation by $d_{50ss}$, (g) *Parker et al.* [1982] equation by $d_i$ (hiding function defined by *Parker et al.* [1982], and (h) *Parker et al.* [1982] equation by $d_i$ (hiding function defined by *Andrews* [1983]).

from flood frequency analyses (section 3) without the uncertainty inherent in field identification of bank-full stage. As $Q_{max}/Q_2$ increases the significance of incorrectly predicting zero transport increases as well. For instance, at the Boise River study site, both variants of the *Meyer-Peter and Müller* [1948] equation incorrectly predicted zero transport rates for approximately 10% of the transport observations. However, because this error occurred for flows approaching only 19% of $Q_2$, only 2% of the cumulative total transport is lost due to this prediction error. The

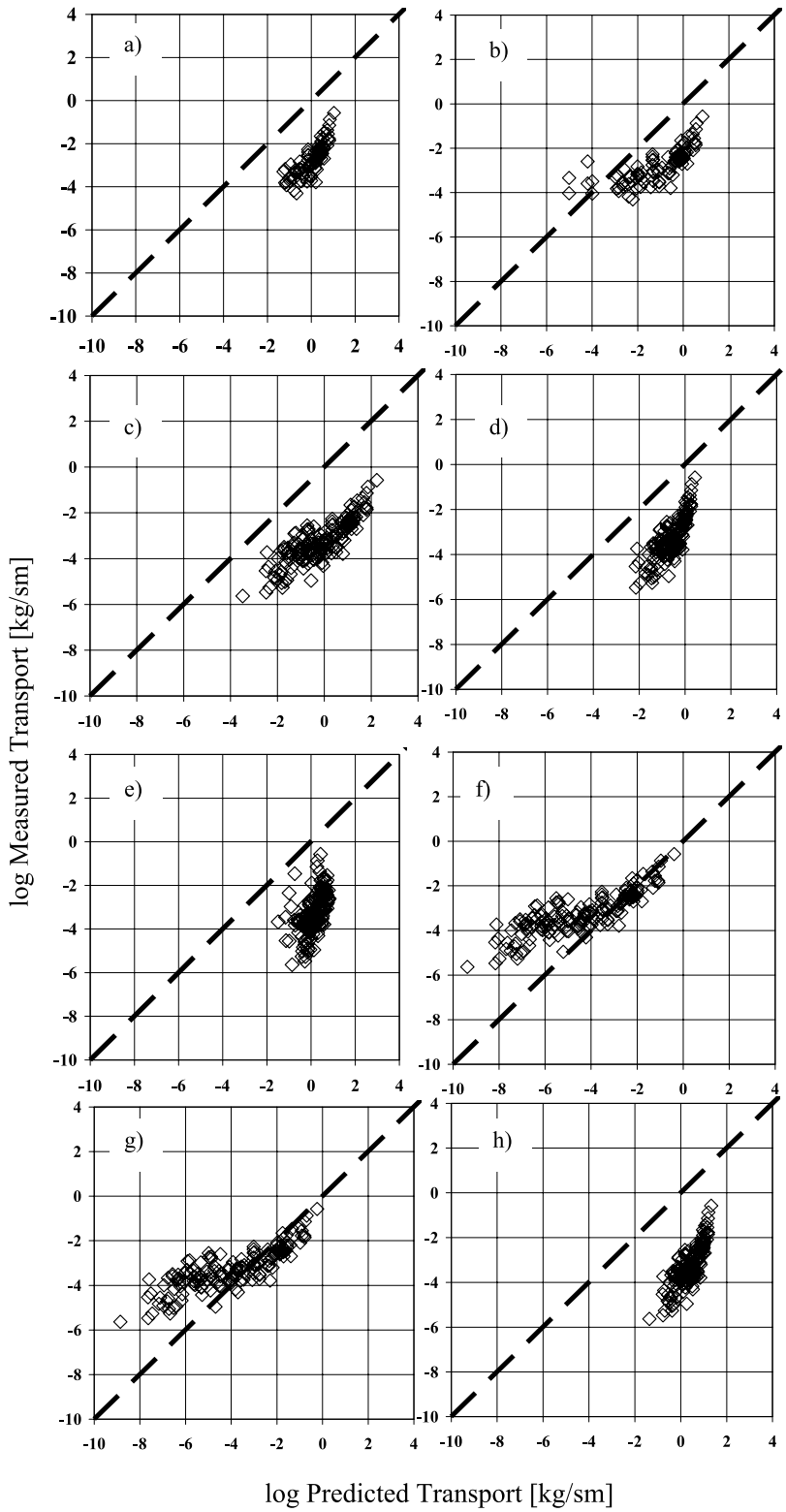


**Figure 2**

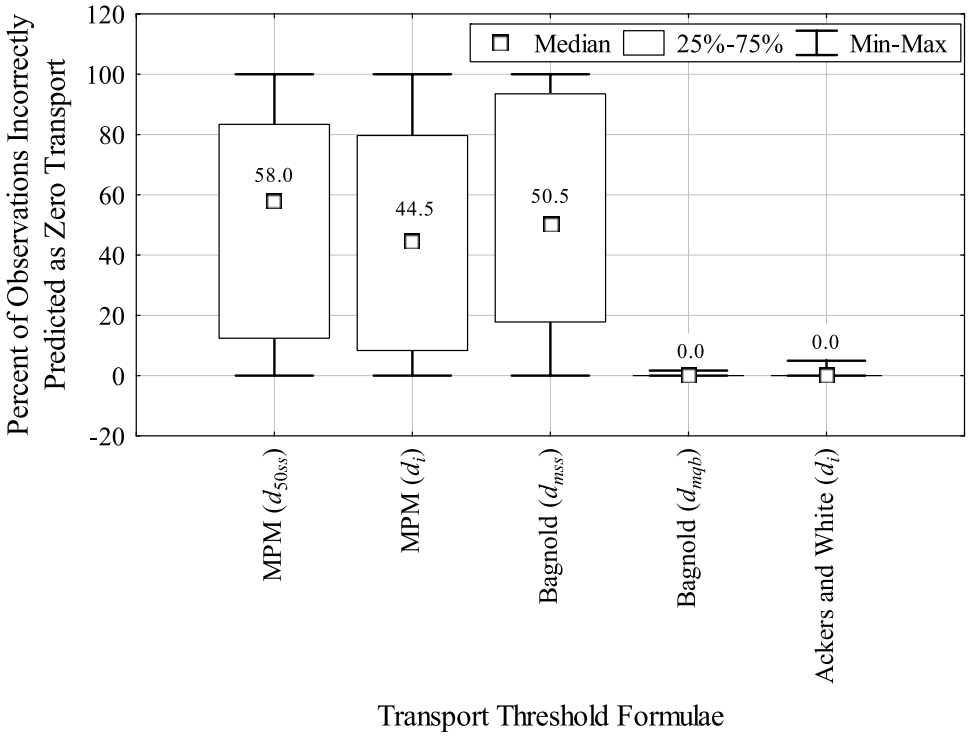


**Figure 3.** Box plots of the distribution of incorrect predictions of zero transport for the 24 Idaho sites. Median values are specified. MPM stands for Meyer-Peter and Müller.

significance of incorrectly predicting zero transport is greater at Valley Creek where, again, both variants of the *Meyer-Peter and Müller* [1948] equation incorrectly predict zero transport rates for approximately 90% of the transport observations and at flows approaching 75% of $Q_2$. This prediction error translates into a loss of 48% of the cumulative bed load transport.

[28] Box plots of $Q_{\max}/Q_2$ values show that incorrect zero predictions are most significant for the *Meyer-Peter and Müller* [1948] equations and the *Bagnold* [1980] ($d_{mss}$) equation, while the *Bagnold* [1980] ($d_{mqb}$) and *Ackers and White* [1973] equations have few incorrect zero predictions and less significant error (lower $Q_{\max}/Q_2$ ratios) (Figure 4).

[29] Because coarse-grained rivers typically transport most of their bed load at near-bank-full discharges [e.g., *Andrews and Nankervis*, 1995], failure of the threshold equations at low flows may not be significant in terms of the annual bed load transport. However, our analysis indicates that in some instances the threshold equations fail at moderate to high discharges ($Q_{\max}/Q_2 > 0.8$), potentially excluding a significant portion of the annual bed load transport (e.g., Valley Creek as discussed above). Moreover, the frequency of incorrect zero predictions varies widely by transport formula (Figure 4). To better understand the performance of these equations it is useful to examine the nature of their threshold formulations.

[30] As discussed in section 2, the *Meyer-Peter and Müller* [1948] equation is a power function of the difference between applied and critical shear stresses. A shear stress correction is used to account for channel roughness and to determine that portion of the total stress applied to the bed (Appendix A). However, the *Meyer-Peter and Müller* [1948] stress correction may be too severe, causing the high number of zero-transport predictions. Bed stresses predicted from the *Meyer-Peter and Müller* [1948] method are typically only 60–70% of the total stress at our sites. Moreover, because armored gravel bed rivers tend to exhibit a near-bank-full threshold for significant bed load transport [*Leopold et al.*, 1964; *Parker*, 1978; *Carling*, 1988; *Andrews and Nankervis*, 1995], the range of transporting shear stresses may be narrow, causing transport predictions to be particularly sensitive to the accuracy of stress corrections.

[31] The *Bagnold* [1980] equation is a power function of the difference between applied and critical unit stream powers. The modal grain size of the subsurface material ($d_{mss}$) is typically 32 mm to 64 mm (geometric mean of 45 mm) at our study sites, whereas the modal grain size of the bed load observations varied widely with discharge and was typically between 1.5 mm at low flows and 64 mm during flood flows. Not surprisingly, the *Bagnold* [1980] equation performs well when critical stream power is based on the modal grain size of each measured bed load event ($d_{mqb}$), but not when it is defined from the mode of the subsurface material ($d_{mss}$) (Figures 3 and 4). When calibrated to the observed bed load data, the critical unit stream power scales with discharge such that at low flows when the measured bed load is fine (small $d_{mqb}$) the critical stream power is reduced. Conversely, as discharge increase and the measured bed load data coarsens (larger $d_{mqb}$) the critical unit stream power increases. However, the mode of the subsurface material ($d_{mss}$) does not scale with discharge and consequently the critical unit discharge is held constant for all flow conditions when based on $d_{mss}$. Consequently, threshold conditions for transport based on $d_{mss}$ are often not exceeded, while those of $d_{mqb}$ were exceeded over 90% of the time.

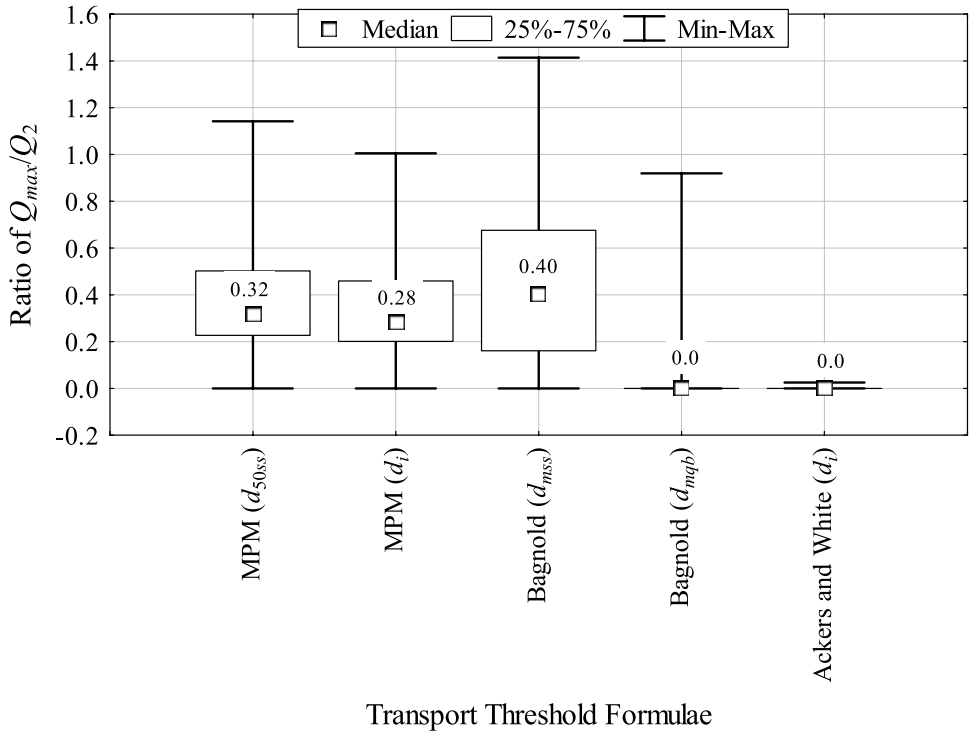


**Figure 4.** Box plots of the distribution of $Q_{\max}/Q_2$ (maximum discharge at which each threshold-based transport formula predicted zero transport normalized by the 2-year flood discharge) for the 24 Idaho sites. Median values are specified. MPM stands for Meyer-Peter and Müller.

[32] In contrast, the *Ackers and White* [1973] equation is a power function of the ratio of applied to critical shear stress minus 1, where the critical shear stress is, in part, a function of $d_{50ss}$, rather than $d_{mss}$. At the Idaho sites, $d_{50ss}$ is typically about 20 mm, and therefore the critical shear stress is exceeded at most flows, resulting in a low number of incorrect zero predictions (Figure 3).

#### 4.1.3. Statistical Assessment

[33] The performance of each formula was also assessed statistically using the $\log_{10}$-difference between predicted and observed total bed load transport. To include the incorrect zero predictions in this analysis we added a constant value, e, to all observed and predicted transport rates prior to taking the logarithm. The lowest nonzero transport rate predicted for the study sites ($1 \times 10^{-15}$ kg $m^{-1}$ $s^{-1}$) was chosen for this constant.

[34] Formula performance changes significantly compared to that of section 4.1.1 when we include the incorrect zero-transport predictions. The distribution of $\log_{10}$ differences across all 24 study sites from each formula is shown in Figure 5. Both versions of the *Meyer-Peter and Müller* [1948] equation and the *Bagnold* [1980] ($d_{mss}$) equation typically underpredict total transport due to the large number of incorrect zero predictions, with the magnitude of this underprediction set by e. All other equations included in this analysis have few, if any, incorrect zero predictions and tend to predict total transport values within 2 to 3 orders of magnitude of the observed values.

[35] To further examine formula performance, we conducted paired sample $c^2$ tests to compare observed versus predicted transport rates for each equation across the 24 study sites. We use *Freese*'s [1960] approach, which differs slightly from the traditional paired sample $c^2$ analysis in that the $c^2$ statistic is calculated as

$$c^2 = \frac{\sum_{i=1}^{n} (x_i - m_i)^2}{s^2} \tag{1}$$

where $x_i$ is the $i$th predicted value, $m_i$ is the $i$th observed value, $n$ is the number of observations, and $s^2$ is the required accuracy defined as

$$s^2 = \frac{E^2}{(1.96)^2} \tag{2}$$

where $E$ is the user-specified acceptable error, and 1.96 is the value of the standard normal deviate corresponding to a two-tailed probability of 0.05. We evaluate $c^2$ using log-transformed values of bed load transport, with e added to both $x_i$ and $m_i$ prior to taking the logarithm, and $E$ defined as one log unit (i.e., ± an order of magnitude error).

[36] *Freese*'s [1960] $c^2$ test shows that none of the equations perform within the specified accuracy (± an order of magnitude error, a = 0.05). Nevertheless, some equations are clearly better than others (Figure 5). To further quantify equation performance, we calculated the critical error, $e^*$, at each of the 24 study sites (Figure 6), where $e^*$ is the smallest value of $E$ that will lead to adequate model performance (i.e., acceptance of the null hypothesis of equal distributions of observed and predicted bed load transport rates assessed via *Freese*'s [1960] $c^2$ test). Hence we are asking how much error would have to be tolerated to accept

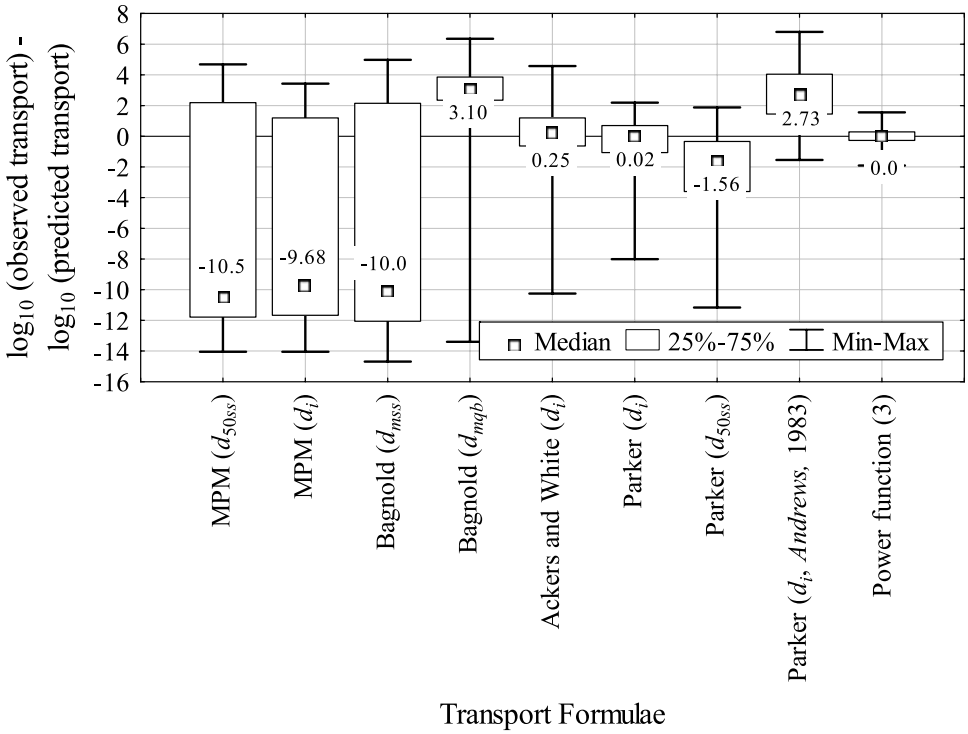


**Figure 5.** Box plots of the distribution of $\log_{10}$ differences between observed and predicted bed load transport rates for the 24 Idaho study sites. Median values are specified. MPM stands for Meyer-Peter and Müller. Power function is discussed in section 4.3.

a given model (bed load transport equation) [*Reynolds*, 1984].

[37] Results show that at best, median errors of less than 2 orders of magnitude would have to be tolerated for acceptance of the best performing equations (*Ackers and White*'s [1973] and *Parker et al.*'s [1982] ($d_i$) equations), while at worst, median errors of more than 13 orders of magnitude would have to be tolerated for acceptance of the

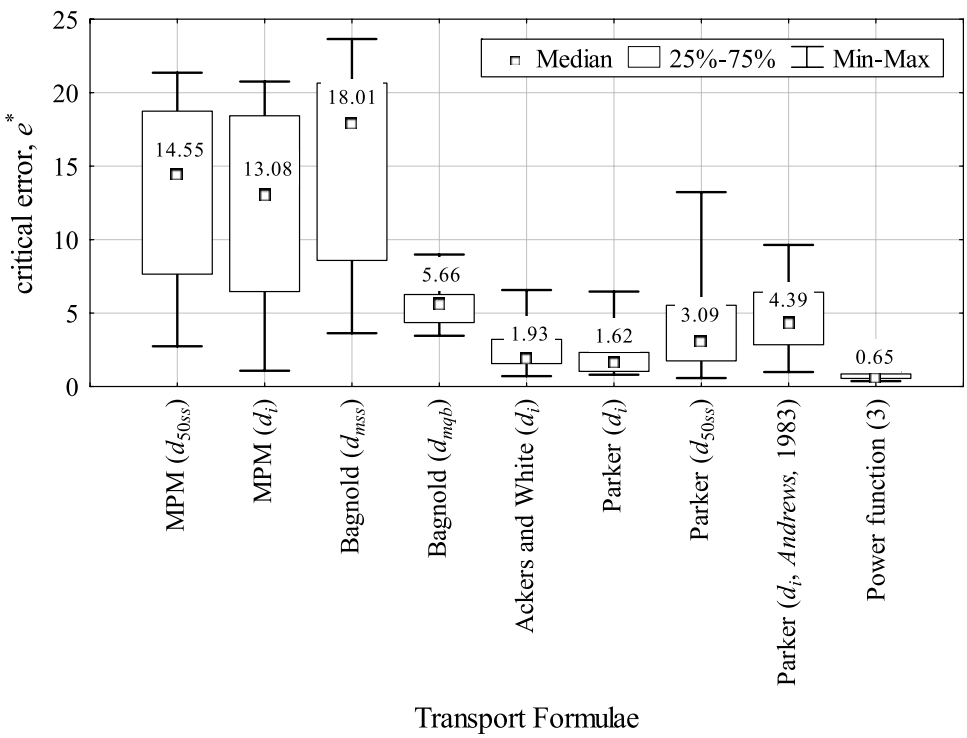


**Figure 6.** Box plots of the distribution of critical error, $e^*$, for the 24 Idaho sites. Median values are specified. MPM stands for Meyer-Peter and Müller. Power function is discussed in section 4.3.

poorest performing equations (Figure 6). In detail, we find that the *Parker et al.* [1982] ($d_i$) equation outperformed all others except for the *Ackers and White* [1973] formula (paired $c^2$ test of $e^*$ values, a = 0.05). However, the median critical errors of these two equations were quite poor (1.62 and 1.93, respectively). The *Bagnold* [1980] ($d_{mss}$) equation and both variants of the *Meyer-Peter and Müller* [1948] equation had the largest critical errors, with the latter not statistically different from one another (paired $c^2$ test, a = 0.05). The *Parker et al.* [1982] ($d_{50ss}$) and the *Parker et al.* [1982] ($d_i$ via *Andrews* [1983]) equations were statistically similar to each other and performed better than the *Bagnold* [1980] ($d_{mqb}$) equation (paired $c^2$ test, a = 0.05).

[38] Although the $c^2$ statistic is sensitive to the magnitude of e, specific choice of e between $1 \times 10^{-15}$ and $1 \times 10^{-7}$ kg m$^{-1}$ s$^{-1}$ does not change the relative performance of the equations or the significance of the differences in performance between them. Nor does it alter the finding that none of the median critical errors, $e^*$, are less than or equal to $E$; the formulae with the lowest critical errors have little to no incorrect zero transport predictions and are thus least affected by e (see Figures 3 and 6).

[39] It should be noted that our analysis of performance does not weight transport events by their proportion of the annual bed load transport (in the sense of *Wolman and Miller* [1960]), but by the number of transport observations. Because there are more low-flow transport events than high-flow ones during a given period of record, the impact of the low-flow events (and any error associated with them) is emphasized. This analysis artifact is common to all previous studies that have examined the performance of bed load transport equations. Hence geomorphic performance (in the sense of *Wolman and Miller* [1960]) remains to be tested in future studies.

### 4.2. Effects of Formula Calibration and Complexity

[40] Accuracy was also considered in relation to degree of formula calibration and complexity. The number and nature of calibrated parameters determines the degree of formula calibration which, in turn, determines equation complexity. In general, formulae computed by grain size fraction ($d_i$), using site-specific particle size distributions, are more calibrated and more complex than those determined from a single characteristic particle size. Moreover, formulae that are fit to observed bed load transport rates and that use site-specific hiding functions (e.g., the *Parker et al.* [1982] ($d_i$) equation) are more calibrated and complex than those that that use a hiding function derived from another site (e.g., our use of the *Andrews* [1983] function in variants of the *Parker et al.* [1982] and *Meyer-Peter and Müller* [1948] equations). The *Bagnold* [1980] formula does not contain a hiding function, is based on a single grain size, has a limited number of user-calibrated parameters and is therefore ranked lowest in terms of both calibration and complexity. However, we have ranked the *Bagnold* [1980] ($d_{mqb}$) variant higher in terms of calibration because the modal grain size varied with discharge and was calculated from the observed bed load transport data. We consider the *Ackers and White* [1973] equation equal in terms of calibration and complexity to both the *Meyer-Peter and Müller* [1948] ($d_i$) equation and the *Parker et al.* [1982] ($d_i$ via *Andrews* [1983]) equation because all three are calculated by $d_i$, have a similar number of calibrated parameters and contain "off the shelf" particle-hiding functions that are calibrated to other sites, rather than to site-specific conditions.

[41] Results from our prior analyses (Figures 5 and 6) indicate that the most complex and calibrated equation (i.e., *Parker et al.* [1982] ($d_i$)) outperforms all other formulae except for the *Ackers and White* [1973] equation. However, we find no consistent relationship between formula performance and degree of calibration and complexity. Size-specific formulae (those calculated by $d_i$) do not consistently outperform those based on a single characteristic particle size ($d_{50ss}$, $d_{mqb}$ or $d_{\mathrm{mss}}$), nor does a site-specific hiding function (i.e., *Parker et al.* [1982] ($d_{50ss}$)) guarantee better performance than an "off the shelf" hiding function (i.e., *Parker et al.* [1982] ($d_i$) via *Andrews* [1983]).

### 4.3. A New Bed Load Transport Equation

[42] The bed load equations examined in sections 4.1 and 4.2 are some of the most common and popular equations used for gravel bed rivers. However, their performance is disconcerting and makes us ask whether there is a better alternative?

[43] Similar to *Whiting et al.* [1999], we find that bed load transport at our sites is generally well described in $\log_{10}$ space ($0.50 < r^2 < 0.90$) by a simple power function of total discharge ($Q$)

$$q_b = \mathrm{a}Q^{\mathrm{b}} \tag{3}$$

where $q_b$ is bed load transport per unit width, and a and b are empirical values [*Leopold et al.*, 1964; *Smith and Bretherton*, 1972; *Vanoni*, 1975]. Figure 7 shows a sample fit of this function at the Boise River study site. Moreover, we find that equation (3) performs within the accuracy specified in section 4.1.3 (*Freese*'s [1960] $c^2$, a = 0.05) and is superior to the other bed load equations examined in terms of describing the observed transport (Figures 5 and 6). In particular, the median critical error, $e^*$, for equation (3) is significantly lower than that of the other equations (paired $c^2$ test, a = 0.05) and is within the specified accuracy ($E$ = 1 $\log_{10}$ unit). We expect this result because equation (3) is empirically fit to the data and thus fully calibrated. Nevertheless, the results demonstrate that a power function of discharge may be a viable alternative to the other equations examined in sections 4.1 and 4.2. To generalize equation (3) and make it predictive, we next parameterize a and b in terms of channel and watershed characteristics.

### 4.4. Parameterization of the Bed Load Transport Equation

[44] We hypothesize that the exponent of equation (3) is principally a factor of supply-related channel armoring. *Emmett and Wolman* [2001] discuss two types of supply limitation in gravel bed rivers. First, the supply of fine material present on the streambed determines, in part, the magnitude of phase I transport (motion of finer particles over an immobile armor) [*Jackson and Beschta*, 1982]. Second, supply limitation occurs when the coarse armor layer limits the rate of gravel transport until the larger particles that make up the armor layer are mobilized thus exposing the finer subsurface material to the flow (phase II transport [*Jackson and Beschta*, 1982]). Mobilization of the surface material in a well armored channel is followed by a

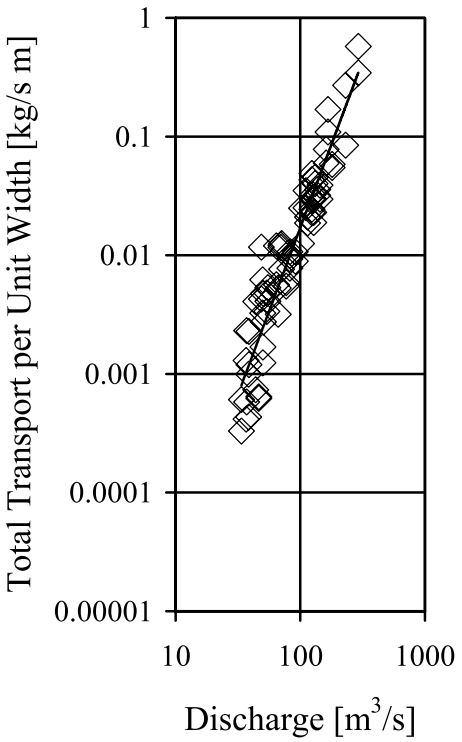


**Figure 7.** Example bed load rating curve from the Boise River study site ($q_b = 4.1 \times 10^{-8}Q^{2.81}$, $r^2 = 0.90$).

relatively larger increase in bed load transport rate compared to a similar channel with less surface armoring. Consequently, we expect that a greater degree of channel armoring, or supply-limitation, will delay mobilization of the armor layer and result in a steeper bed load rating curve (larger exponent of the bed load equation (3)) compared to a less armored channel [*Emmett and Wolman*, 2001].

[45] *Dietrich et al.* [1989] proposed that the degree of channel armoring is related to the upstream sediment supply relative to the local transport capacity, and presented a dimensionless bed load transport ratio, $q^*$, to represent this relationship. Here, we use $q^*$ as an index of supply-related channel armoring and examine its effect on the exponent (b) of the observed bed load rating curves (3).

[46] We define $q^*$ as

$$q^* = \left(\frac{\tau_{Q_2} - \tau_{d_{50s}}}{\tau_{Q_2} - \tau_{d_{50ss}}}\right)^{1.5} \tag{4}$$

where $\tau_{Q_2}$ is the total shear stress at $Q_2$ calculated from the depth-slope product ($\rho gDS$, where $\rho$ is fluid density, $g$ is gravitational acceleration, $D$ is flow depth at $Q_2$ calculated from hydraulic geometry relationships, and $S$ is channel slope) and $\tau_{d_{50s}}$ and $\tau_{d_{50ss}}$ are the critical shear stresses necessary to mobilize the surface and subsurface median grain sizes, respectively. Channel morphology and bed load transport are adjusted to bank-full flows in many gravel bed rivers [e.g., *Leopold et al.*, 1964; *Parker*, 1978; *Andrews and Nankervis*, 1995], hence bank-full is the relevant flow for determining $q^*$ in natural rivers [*Dietrich et al.*, 1989]. However, we use $Q_2$ because it is a bank-full-like flow that can be determined objectively from flood frequency analyses without the uncertainty inherent in field identification of bank-full stage (section 4.1.2). The critical shear stresses are calculated as

$$\tau_{d_{50s}} = \tau^*_{c50}(\rho_s - \rho)gd_{50s} \tag{5a}$$

$$\tau_{d_{50ss}} = \tau^*_{c50}(\rho_s - \rho)gd_{50ss} \tag{5b}$$

where $\tau^*_{c50}$ is the dimensionless critical Shields stress for mobilization of the median grain size. We set this value equal to 0.03, corresponding with the lower limit of dimensionless critical Shield stress values for visually based determination of incipient motion in coarse-grained channels [*Buffington and Montgomery*, 1997].

[47] Values for $q^*$ range from 0 for low bed load supply and well-armored surfaces ($d_{50s} \gg d_{50ss}$ and $\tau_{d_{50s}} \approx \tau_{Q_2}$) to 1 for high bed load supply and unarmored surfaces ($d_{50s} \approx d_{50ss}$ and $\tau_{d_{50s}} \approx \tau_{d_{50ss}}$). As demonstrated by *Dietrich et al.* [1989], $q^*$ does not measure absolute armoring (i.e., it is not uniquely related to $d_{50s}/d_{50ss}$), but rather relative armoring (a function of transport capacity relative to bed load supply). The denominator of (4) is the equilibrium transport capacity of the unarmored bed and is a reference transport rate (theoretical end-member) that quantifies the maximum bed load transport capacity for the imposed boundary shear stress and the size of supplied bed load material. The numerator is the equilibrium transport rate for the actual bed load supply (equilibrium excess shear stress), with equilibrium transport achieved by textural adjustment of the bed (fining or coarsening in response to bed load supply) [e.g., *Dietrich et al.*, 1989; *Buffington and Montgomery*, 1999b]. Hence $q^*$ is a relative index of armoring (textural adjustment as a function of excess shear stress that provides equilibrium bed load transport). It describes armoring as a function of bed load supply relative to boundary shear stress and transport capacity. Consequently, $q^*$ is not a measure of absolute armoring ($d_{50s}/d_{50ss}$). For the same degree of armoring, one can have different values of $q^*$, depending on the bed load supply and the corresponding equilibrium excess shear stress [*Dietrich et al.*, 1989; *Lisle et al.*, 2000]. Similarly, for a given $q^*$, a lower degree of armoring will occur for lower values of equilibrium excess shear stress [*Dietrich et al.*, 1989; *Lisle et al.*, 2000].

[48] We determined values of $q^*$ at 21 of the 24 study sites. Values of $q^*$ could not be determined for three of the study sites because their median grain sizes were calculated to be immobile during $Q_2$ (Salmon River at Shoup, Middle Fork Salmon River at Lodge and Selway River). Results show an inverse relationship between $q^*$ and the exponent of our bed load power function (Figure 8) supporting the hypothesis that supply-related changes in armoring relative to the local transport capacity influence the delay in bed load transport and the slope of the bed load rating curve. We parameterize $q^*$ in terms of low-flow bed material for practical reasons (safety during grain size measurement and feasibility of future application of our approach). However, surface grain size can change with discharge and transport rate [*Parker and Klingeman*, 1982; *Parker et al.*, 2003], thereby potentially making b discharge dependent. Nevertheless, b is an average value across the range of observed discharges (including channel-forming flows) and

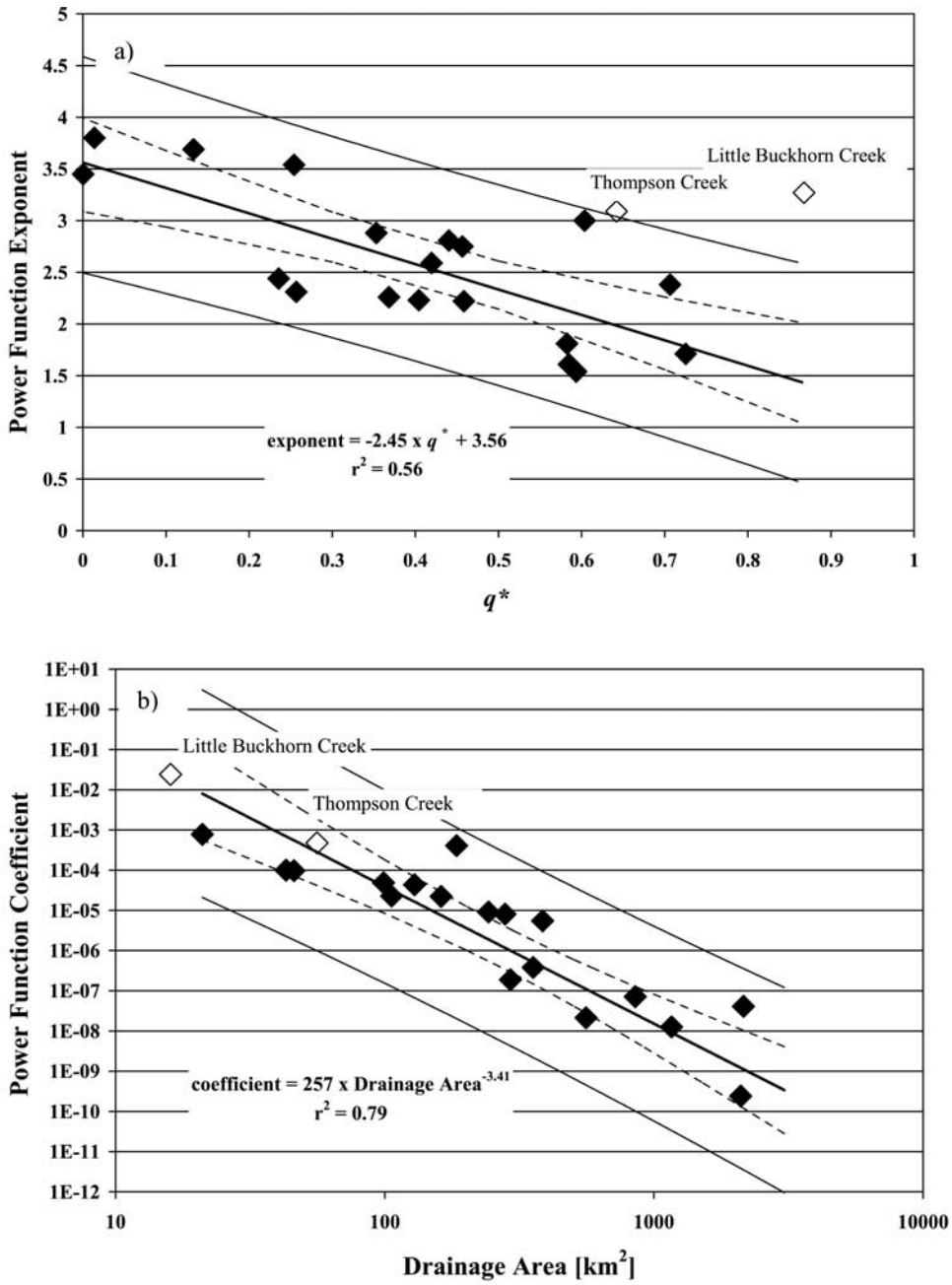


**Figure 8.** Relationships between (a) $q^*$ and the exponent of the bed load rating curves (equation (3)) and (b) drainage area and the coefficient of the bed load rating curves (equation (3)) for the Idaho sites. Dashed lines indicate 95% confidence interval about the mean regression line. Solid lines indicate 95% prediction interval (observed values) [*Neter et al.*, 1974; *Zar*, 1974].

any textural changes are empirically incorporated into our relationship between b and $q^*$.

[49] Two sites (Thompson Creek and Little Buckhorn) appear to be outliers and therefore were removed from the analysis (shown as open diamonds in Figure 8). The anomalous Thompson Creek $q^*$ value may be due to an extensive network of upstream beaver dams. The availability of sediment at all but the greatest flows is likely influenced by dam storage, delaying transport and increasing b by compressing the effective flows into a smaller portion of the hydrograph. In contrast, the large $q^*$ value for Little Buckhorn may be due to a lack of peak flow information. The $Q_2$ at this site was calculated from a drainage area versus $Q_2$ relationship developed from the other 23 Idaho study sites where peak flow information was available. This relationship may overpredict $Q_2$ at Little Buckhorn, resulting in an anomalously high $q^*$ value.

[50] Because $q^*$ is a relative measure of armoring (i.e., relative to bed load supply and transport capacity), it is unlikely to be biased by site-specific conditions (climate, geology, channel type, etc.). For example, the relative nature of $q^*$ implies that channels occurring in different physiographic settings and possessing different particle size distributions (e.g., a fine gravel bed stream versus a coarse

cobble bed one) may have identical values of $q^*$, indicating identical armoring conditions relative to transport capacity and bed load sediment supply and thus identical bed load rating curve slopes. Although, $q^*$ is not uniquely related to absolute armoring ($d_{50s}/d_{50ss}$), we examined its effect on the exponent of our transport function (3), and found that the relationship was not significant ($F$ test, a = 0.05). Hence relative armoring ($q^*$) is more important than absolute armoring ($d_{50s}/d_{50ss}$). Because $q^*$ is a relative index of armoring, it should be a robust predictor of the exponent of our bed load power function and unbiased by changing physiography and channel morphology.

[51] In contrast, the coefficient of the bed load power function (a) describes the absolute magnitude of bed load transport, which is a function of basin-specific sediment supply and discharge. In general, sediment transport rate ($q_b$) and discharge ($Q$) both increase with drainage area ($A$) [*Leopold et al.*, 1964], however discharge increases faster, such that the coefficient of the bed load power function is inversely related to drainage area (a surrogate for transport rate relative to discharge, a $\propto$ $1/A \propto q_b/Q$) (Figure 8). The rate of downstream increase in unit bed load transport rate ($q_b$) also depends on 1) downstream changes in channel width (a function of discharge, riparian vegetation, geology and land use) and 2) loss of bed load material to the suspended fraction due to particle abrasion [*Cui and Parker*, 2004]. Factors that affect channel width also influence flow depth, boundary shear stress, and surface grain size and thus may influence, and be partially compensated by, b. We hypothesize that the Figure 8 relationship is a region-specific function of land use and physiography (i.e., topography, geology, and climate). Consequently, care should be taken in applying this function to other regions. In contrast, prediction of the exponent of our bed load transport equation may be less restrictive, as discussed above.

[52] On the basis of the relationships shown in Figure 8 we propose the following empirically derived total bed load transport function with units of dry mass per unit width and time (kg m$^{-1}$ s$^{-1}$).

$$q_b = 257\ A^{-3.41} Q^{\left(-2.45q^* + 3.56\right)} \tag{6}$$

where the coefficient and exponent are parameterized in terms of channel and watershed characteristics. The coefficient is a power function of drainage area (a surrogate for the magnitude of basin-specific bed load supply) and the exponent is a linear function of $q^*$ (an index of channel armoring as a function of transport capacity relative to bed load supply).

[53] The 17 independent test sites (Table 1) allow us to consider two questions concerning our bed load equation (6). First, how well can we predict the coefficient and exponent of the bed load power function at other sites? Second, how does our bed load formula perform relative to those examined in section 4.1? These questions are addressed in the next two sections.

### 4.5. Test of Equation Parameters

[54] We test our parameterization of equation (6) by comparing predicted values of the formula coefficient (a) and exponent (b) to observed values at 17 independent test sites in Wyoming, Colorado and Oregon (Figure 1). The independent test sites cover a generally similar range of slopes and particle sizes as the 24 Idaho sites used to develop equation (6) (Table 1). However, the East Fork River test site occurs at the gravel/sand transition [e.g., *Sambrook Smith and Ferguson*, 1995; *Ferguson et al.*, 1998; *Parker and Cui*, 1998] and is significantly finer than the coarse-grained Idaho study sites. The Idaho study sites and the supplemental test sites are all snowmelt-dominated streams, except for Oak Creek which is a rainfall-dominated channel. The geology is also similar across the study and test sites. The channels are predominantly underlain by granitics, with some metamorphic and sedimentary geologies, except for Oak Creek which is underlain by basalt. Bed load transport was measured with Helley-Smith samplers at all sites, with the exception of the East Fork and Oak Creek sites, where slot traps were used [*Milhous*, 1973; *Leopold and Emmett*, 1997].

[55] As expected, the exponent of our bed load function is better predicted on average at the 17 test sites than the coefficient (Figure 9). The observed exponents are reasonably well predicted by equation (6) with a median error of less than 3%. This suggests that $q^*$, determined in part through measurements of the surface and subsurface material during low flow, is able to accurately predict the rating curve exponent over a range of observed discharges (including channel-forming flows) despite any stage-dependent changes in surface grain size [*Parker and Klingeman*, 1982; *Parker et al.*, 2003]. Moreover, the rating curve exponents are accurately predicted across different climatic regimes (snowmelt- and rainfall-dominated), different lithologies (basalt and granite), and different bed load sampling methods (Helley-Smith and slot samplers), despite the fact that the predictive equation is derived from a subset of these conditions (i.e., snowmelt rivers in granitic basins, sampled via Helley-Smith). In particular, b is reasonably well predicted at the two test sites that are most different from the Idaho study sites (Oak Creek and East Fork; observed b values of 2.55 and 2.19 versus predicted values of 2.43 and 1.82, respectively). We suspect that the success of our exponent function is due to the robust nature of $q^*$ to describe supply-related channel armoring regardless of differences in physiography and channel conditions (section 4.4).

[56] In contrast, the predicted coefficients are considerably less accurate and were over 3 times larger than the observed values at many of the 17 test sites (Figure 9). Prediction errors, however, can be significant for both parameters, which is expected given the spread of the 95% prediction intervals shown in Figure 8. The largest errors in predicting the coefficient occurred at the Oak Creek and East Fork sites (3 orders of magnitude overprediction, and 2 orders of magnitude underprediction, respectively). The cause of the error at these sites is examined below.

[57] The Oak Creek watershed is unique relative to the 24 Idaho study sites in that it is composed primarily of basalt, rather than granite, and has a climatic regime dominated by rainfall, rather than snowmelt. Because equation (6) accurately predicts the exponent of the Oak Creek bed load rating curve, as discussed above, the overprediction of total bed load transport at this site is principally due to prediction error of the transport coefficient

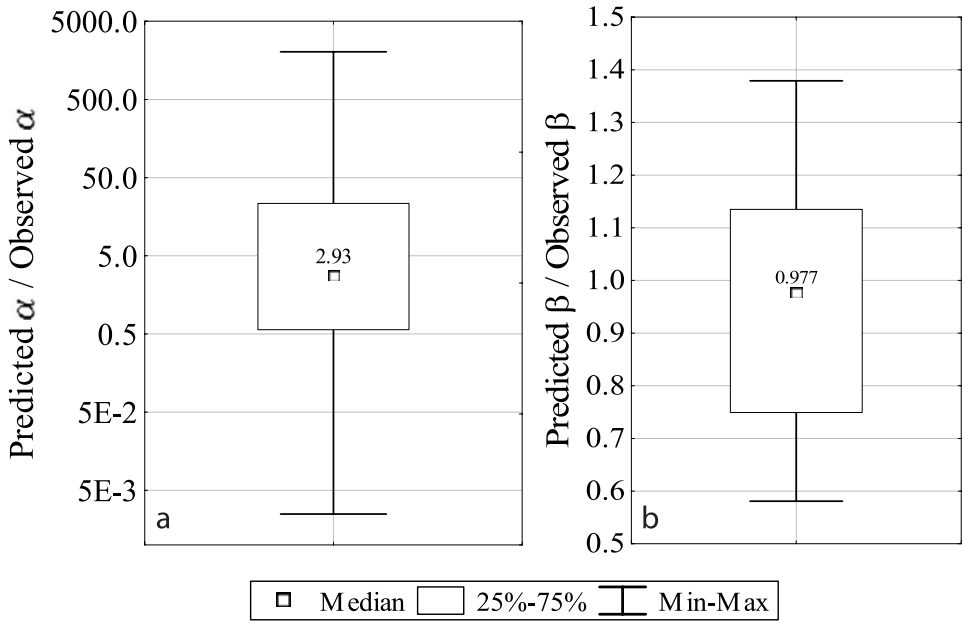


**Figure 9.** Box plots of predicted versus observed values of (a) coefficient and (b) exponent of our bed load transport function (6). Median values are specified.

(observed a of $1.9 \times 10^{-4}$ versus predicted a of 0.39), which may be due to differences in basin geology and sediment production rates. Basalt is typically less erosive and produces less sediment per unit area than the highly decomposed granites found in the Idaho batholith [e.g., *Lisle and Hilton*, 1999]. Consequently, one would expect equation (6) to overpredict the transport coefficient at Oak Creek, as observed. Alternatively, the bed load supply and transport coefficient may be influenced by climate and runoff regime; however the relationship between these two variables is not well documented. Previous studies suggest that in temperate climates bed load supplies may be higher in rainfall regimes than snowmelt-dominated ones [*Lisle et al.*, 2000]. Therefore our a prediction, which is derived from snowmelt streams, would be expected to underpredict transport rates in the rainfall-dominated Oak Creek, contrary to what we observe. Consequently, differences in runoff regime do not appear to explain the observed error at Oak Creek. Regardless of the exact physical cause, the prediction error highlights the site-specific nature of our coefficient function (a) (discussed further in section 4.7).

[58] In contrast, the underprediction of the transport coefficient at East Fork may be due to a difference in channel type. The East Fork site occurs at the gravel/sand transition and has a finer, more mobile bed than the coarser-grained Idaho sites. The gravel/sand transition represents a shift in the abundance of sand-sized material that likely increases the magnitude of phase I transport and total sediment load compared to gravel bed channels. Consequently, one might expect equation (6) to underpredict the coefficient at East Fork, as observed.

[59] The Oak Creek and East Fork sites also differ from the others in that bed load samples were obtained from channel-spanning slot traps, rather than Helley-Smith samplers. Recent work by *Bunte et al.* [2004] shows that differences in sampling method can dramatically affect bed load transport results, although *Emmett* [1980] demonstrates reasonably good agreement between slot and Helley-Smith samples at the East Fork site. Consequently, differences in sampling method do not explain the observed prediction error of the transport coefficient, at least at the East Fork site.

[60] Differences in climate and runoff regime may also influence the rating curve exponent (b). This is not a source of error in our analysis (b is accurately predicted by equation (6), even at Oak Creek), but rather a source of systematic variation in b. A rainfall-dominated climate produces greater short-term variability in the annual hydrograph (i.e., flashier hydrograph) than one dominated by snowmelt [*Swanston*, 1991; *Lisle et al.*, 2000] and typically generates multiple peak flows throughout the year versus the single, sustained peak associated with spring snowmelt. Consequently, the frequency and magnitude of bed load events differs between rainfall- and snowmelt-dominated hydrographs. The magnitude of flow associated with a given return period is typically greater in a rainfall-dominated watershed than in a similarly sized snowmelt-dominated watershed [*Pitlick*, 1994]. This is seen at our study sites in that the highest $Q_2$ unit discharge (0.44 $m^3$ $km^{-2}$) occurs at the rainfall-dominated Oak Creek test site and is almost twice the second highest $Q_2$ unit discharge (0.27 $m^3$ $km^{-2}$) at the snowmelt-dominated Dollar Creek study site. Furthermore, because of the greater short-term variability of rainfall-dominated hydrographs, the duration of intermediate flows is reduced, which can lead to fining of the bed surface and a decrease in the degree of the channel armoring [*Laronne and Reid*, 1993; *Lisle et al.*, 2000; *Parker et al.*, 2003]. Consequently, one might expect less armoring and lower bed load rating curve exponents (b) in rainfall-dominated environments compared to snowmelt ones. However, b and the degree of armoring are also influenced by bed load supply and boundary shear stress (section 4.4),

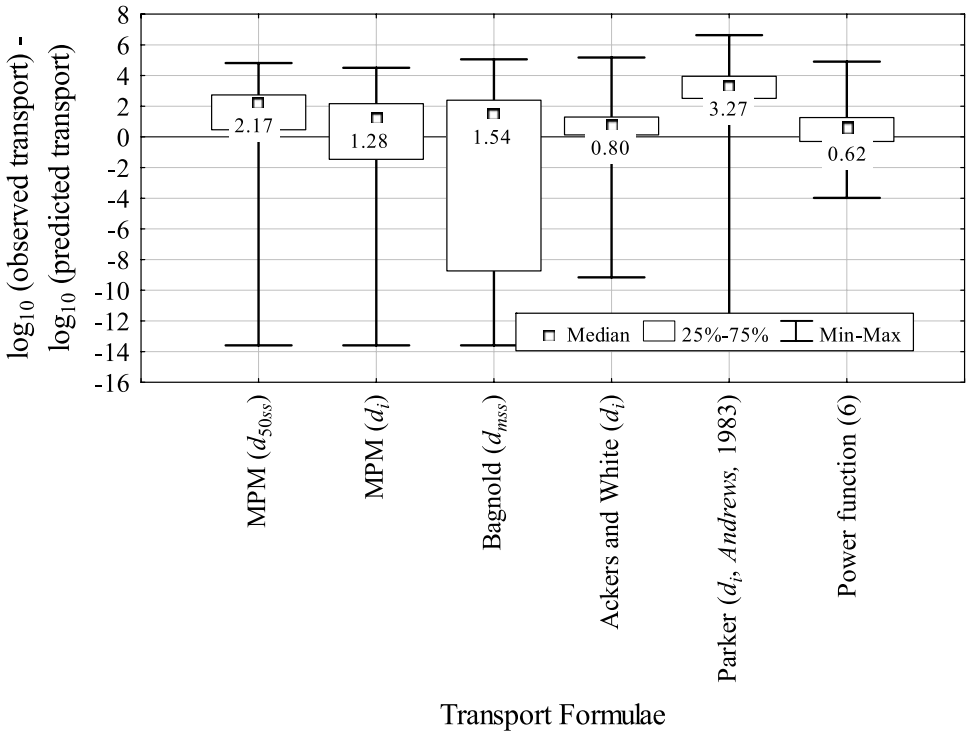


**Figure 10.** Box plots of the distribution of $\log_{10}$ differences between observed and predicted bed load transport rates at the 17 test sites. Median values are specified. MPM stands for Meyer-Peter and Müller.

so those parameters must be factored into any comparison of runoff regimes. Lack of data (only one rainfall-dominated site in our data set) precludes further examination of this issue here.

### 4.6. Comparison With Other Equations

[61] To compare the accuracy of our bed load transport equation (6) to those presented in section 4.1, we performed a test of six formulae (including equation (6)) at the 17 test sites. The test procedure was similar to that used in section 4.1.3; however, we assume no transport observations are available for formula calibration (i.e., blind test), and therefore we do not include the two variants of the *Parker et al.* [1982] ($d_i$ and $d_{50ss}$) equation or the *Bagnold* [1980] ($d_{mqb}$) equation which require measured bed load transport data. Consequently, only five of the eight variants of the formulae from section 4.1 are included here, plus our power law equation (6).

[62] Similar to section 4.1, incorrect zero-transport predictions are a problem for threshold-based equations, but the number of zero predictions is significantly less at the test sites (about 50% less compared to those shown in Figure 3 for the Idaho study sites). For both variants of the *Meyer-Peter and Müller* [1948] equation the median percentage of incorrect zero transport predictions is about 22%, while the median percentage of incorrect zero predictions for the *Bagnold* [1980] ($d_{mss}$) equation is 28%. In contrast, the *Ackers and White* [1973] equation incorrectly predicted zero transport at only one test site (Oak Creek) for 35% of the observations. The significance of incorrect zero-transport predictions is similar at the 17 test sites as at the 24 Idaho sites. The $Q_{\max}/Q_2$ ratio for both variants of the *Meyer-Peter and Müller* [1948] ($d_{50ss}$ and $d_i$) equation had a median value of 29% and 26%, respectively, at the Idaho sites and about 30% at the test sites. The $Q_{\max}/Q_2$ ratio for the *Bagnold* [1980] ($d_{mss}$) equation decreased slightly from a median value of 40% at the Idaho sites to 27% at the test sites.

[63] Figure 10 shows the distribution of $\log_{10}$ differences across the 17 test sites and demonstrates a significant improvement in the performance of both versions of the *Meyer-Peter and Müller* [1948] equation and the *Bagnold* [1980] ($d_{mss}$) equation due to fewer incorrect zero transport predictions; median $\log_{10}$ differences improve from an underprediction of almost 10 orders of magnitude at the 24 Idaho sites to an overprediction of only 1.3 to 2.2 orders of magnitude at the test sites. The performance of both the *Parker et al.* [1982] ($d_i$ via *Andrews* [1983]) equation and the *Ackers and White* [1973] equation decreased slightly at the test sites with median $\log_{10}$ differences increasing from 2.73 and 0.25, respectively, at the Idaho sites to 3.27 and 0.80, respectively, at the test sites. Our bed load equation (6) had the lowest median $\log_{10}$ difference (0.62) at the 17 test sites.

[64] As in section 4.1.3, the performance of each formula was evaluated using *Freese*'s [1960] $c^2$ test, with results similar to those of the Idaho sites; all formulae perform significantly worse than the specified accuracy ($E = 1 \log_{10}$ unit, a = 0.05), including equation (6). We also evaluated the critical error, $e^*$ [*Reynolds*, 1984], at each test site and, like the Idaho study sites, we found that a given formula may occasionally provide the required accuracy, but generally no equation performs within the specified accuracy (Figure 11, all median $e^*$ values $>E$).

[65] Nevertheless, our bed load transport equation (6) outperformed all others at the 17 test sites, except for the

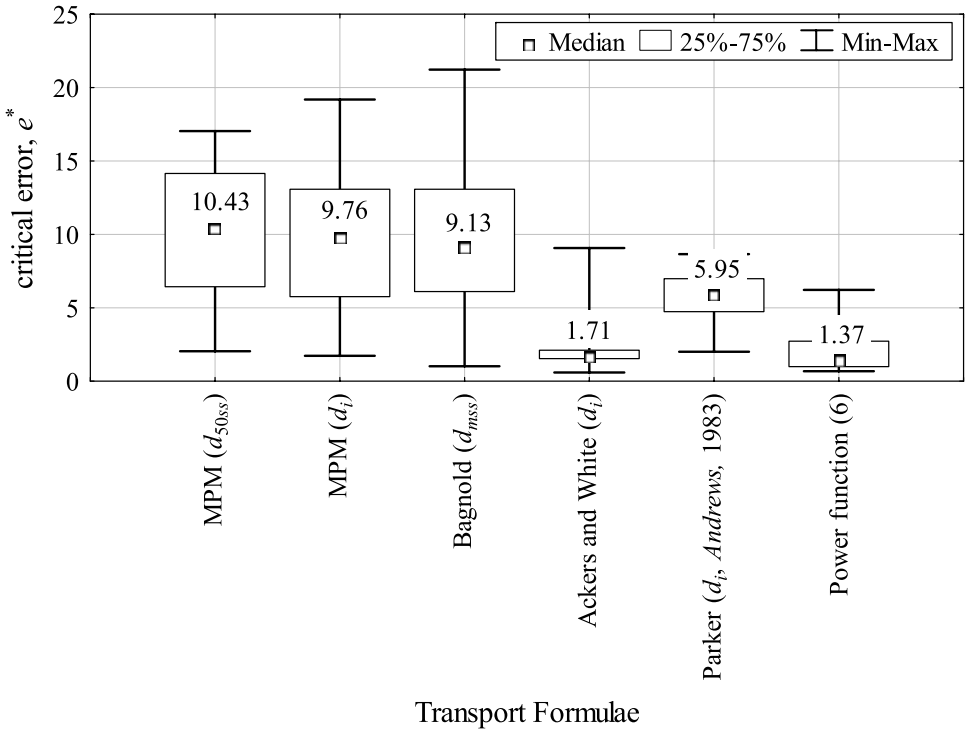


**Figure 11.** Box plots of the distribution of critical error, $e^*$, for the 17 test sites. Median values are specified. MPM stands for Meyer-Peter and Müller.

*Ackers and White* [1973] equation which was statistically similar to ours (paired $c^2$ test of $e^*$ values, a = 0.05) (Figure 11). As with the Idaho sites, the worst performers were the *Bagnold* [1980] ($d_{mss}$) equation and both variants of the *Meyer-Peter and Müller* [1948] equation, both of which were similar to one another, but different from the *Bagnold* [1980] ($d_{mss}$) equation (paired $c^2$ test, a = 0.05). Critical errors for the *Parker et al.* [1982] ($d_i$ via *Andrews* [1983]) equation were between these two groups of best and worst performers and statistically different from them (paired $c^2$ test, a = 0.05). Overall, the patterns of formula performance were similar to those of the Idaho study sites, but the 17 test sites tended to have lower values of critical error (see Figures 6 and 11).

### 4.7. Formula Calibration

[66] A principle drawback of our proposed bed load transport equation (6) appears to be the site-specific nature of the coefficient function (a). However, it may be possible to back calculate a local coefficient from one or more low-flow bed load transport measurements coupled with prediction of the rating curve exponent as specified in equation (6), thus significantly reducing the cost and time required to develop a bed load rating curve from traditional bed load sampling procedures [e.g., *Emmett*, 1980]. A similar approach of formula calibration from a limited number of transport observations was proposed by *Wilcock* [2001]. Our suggested procedure for back calculating the coefficient assumes that the exponent can be predicted with confidence (as demonstrated by our preceding analyses).

[67] By way of example, we used equation (6) to calculate the exponent of the bed load rating curve at Oak Creek and then randomly selected 20 low-flow bed load transport observations to determine 20 possible rating curve coefficients. Low flows are defined as those less than the average annual value. The average predicted coefficient using this calibration method is 0.00032, which is much closer to the observed value (0.00019) than our original prediction (0.39) from equation (6). Thus our calibration method better approximates the observed coefficient. Using the exponent predicted from equation (6) and the calibrated coefficient of 0.00032, we predict total transport for each observation made at Oak Creek. Results show that the critical error, $e^*$, improves from 6.17 to 1.53. Figure 12 illustrates the improved accuracy of our bed load formula with calibration to a limited number of low-flow transport observations.

## 5. Summary and Conclusions

[68] The bed load transport data sets obtained from 24 study sites in central Idaho, USA, provide an opportunity to extend the analyses of *Gomez and Church* [1989] and *Yang and Huang* [2001] into coarse-grained mountain rivers and to continue recent studies of those environments [*Almedeij and Diplas*, 2003; *Bravo-Espinosa et al.*, 2003; *Martin*, 2003]. We evaluated the performance of eight different formulations of four common bed load transport equations, each of which are calibrated to some degree with site-specific data and vary in their complexity and difficulty of use. Although we find considerable differences in formula performance, there is no consistent relationship between performance and degree of formula calibration or complexity at the 24 Idaho sites. However, formulae containing a threshold for bed load transport commonly predict a substantial number of incorrect zero-transport rates and typically perform worse than nonthreshold

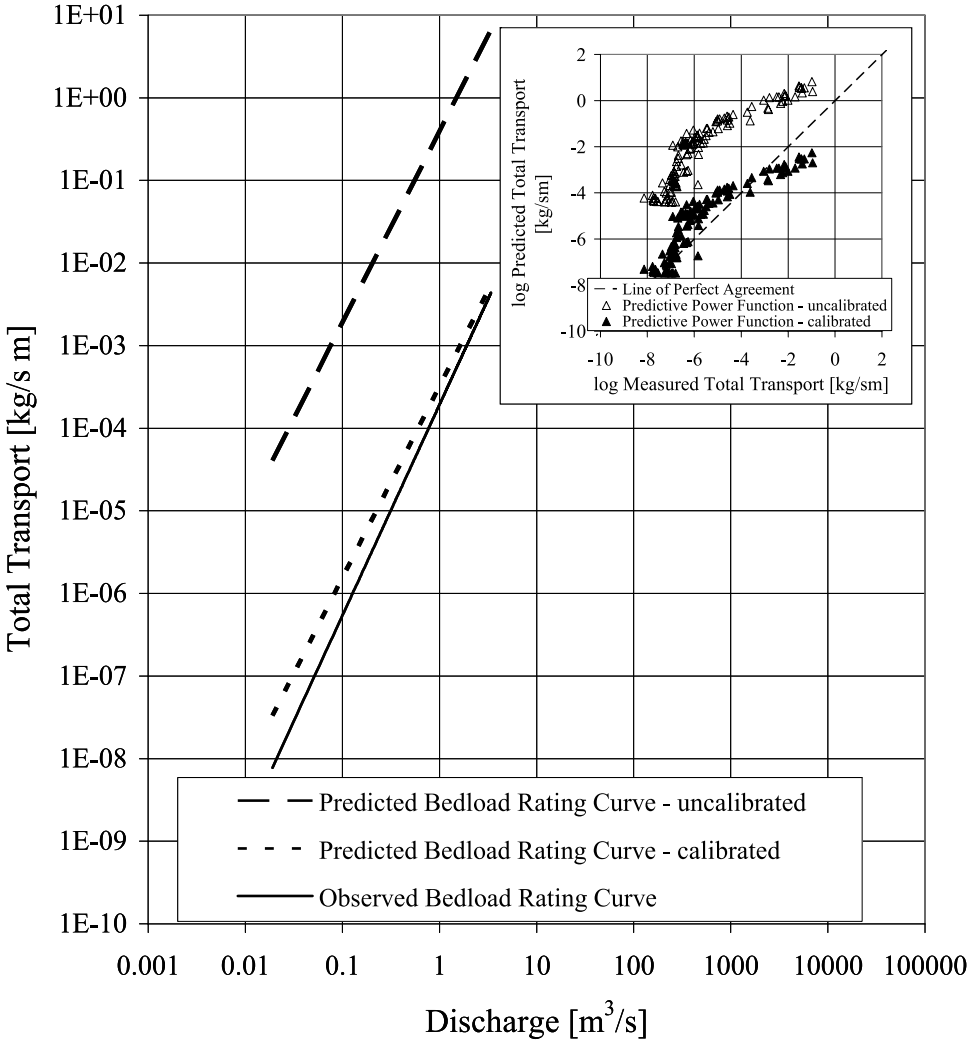


**Figure 12.** Observed versus predicted bed load transport rates at Oak Creek, illustrating improved performance by calibrating the coefficient of our equation (6) to a limited number of observed, low-flow, transport values.

formulae. Moreover, we find that a simple power function of discharge best describes the observed transport at the Idaho sites (*Freese*'s [1960] $c^2$, a = 0.05). This result is expected because the power function is empirically fit to the observed data. Nevertheless, the simplicity of the equation is attractive, and we develop it into a predictive transport equation by parameterizing its coefficient and exponent in terms of channel and watershed conditions at the 24 Idaho study sites.

[69] We find that the exponent of the bed load rating curve is inversely related to $q^*$ which describes the degree of channel armoring relative to transport capacity and sediment supply [*Dietrich et al.*, 1989]. Because $q^*$ is a relative index of supply-limited channel armoring we expect our exponent equation to be transferable to other physiographies and channel types. In contrast, we find that the coefficient of our bed load power function is inversely related to drainage area and is likely a function of site-specific sediment supply and channel type. As such, the coefficient equation may not be as transferable to other locations, but can be locally calibrated (section 4.7). We use an additional 17 independent data sets to test the accuracy of our bed load power function.

[70] As expected, the exponent is better predicted than the coefficient at the 17 independent test data sets, with typical errors of less than 3% and almost 300%, respectively. We find that our coefficient function is sensitive to local geology and channel type. In particular, our bed load formula was developed from watersheds composed principally of granitics and coarse-grained channel types, and when applied to a less erosive lithology, such as basalt (Oak Creek), we tend to overpredict bed load transport. This is due to the site-specific nature of our coefficient function rather than errors associated with our exponent function (at Oak Creek the observed a = $1.9 \times 10^{-4}$, predicted a = 0.39; observed b = 2.55, predicted b = 2.43). Conversely, when we apply our formula to a channel at the gravel/sand transition (East Fork River) we underpredict the amount of bed load transport for a given drainage area, again, due to the site-specific nature of our coefficient function (observed a = $8.26 \times 10^{-5}$, predicted a = $2.06 \times 10^{-7}$; observed b = 2.19, predicted b = 1.82).

[71] Despite these concerns, we find that our bed load formula significantly outperformed three of the four trans-

port formulae examined and was statistically similar to the *Ackers and White* [1973] equation at the 17 independent test sites.

[72] Although our exponent function appears to be robust, a more thorough test of both the coefficient and exponent functions, covering a wider range of geologies and climatic regimes, is warranted. Moreover, our definition of $q^*$ requires stage–discharge data to determine $Q_2$ from flood frequency analyses and to determine the $Q_2$ flow depth from hydraulic geometry relationships. Because the cost and time involved in stream gauging may be prohibitive, an alternative and simpler approach might be to define $q^*$ based on field measurements of bank-full parameters. Bank-full depth can be determined from cross-sectional surveys, and bank-full discharge can be estimated from the *Manning* [1891] equation combined with channel surveys of slope, bank-full radius, and an appropriate estimate of channel roughness [e.g., *Barnes*, 1967].

[73] Our proposed transport equation also has applications for channel maintenance flows [*Whiting*, 2002] which are often based on identifying discharges that transport the most sediment over the long term (i.e., effective flows [*Wolman and Miller*, 1960]). This type of analysis does not require knowledge of the actual amount of sediment in transport, but rather requires only an understanding of how bed load transport changes with discharge (i.e., quantifying the bed load rating curve exponent). Consequently, our bed load formula offers a means to determine the exponent of the rating curve without the time or expense of a full bed load measurement campaign. For example, with the exponent of the bed load rating curve predicted from equation (6), the "effective discharge" can be calculated following the procedure outlined by *Emmett and Wolman* [2001] and does not depend on the coefficient of the bed load rating curve.

[74] The bed load formulae examined here are all one-dimensional equations parameterized by reach-average hydrologic and sedimentologic variables. However, most natural channels exhibit patchy surface textures [e.g., *Kinerson*, 1990; *Paola and Seal*, 1995; *Buffington and Montgomery*, 1999a; *Laronne et al.*, 2000] and spatially variable hydraulics. Moreover, because transport rate is a nonlinear function of excess boundary shear stress, whole-channel transport rates based on reach-average conditions tend to under predict transport rates unless empirically adjusted [*Lisle et al.*, 2000; *Ferguson*, 2003]. Thus predictions of bed load transport rates ultimately would be more accurate and true to processes in natural channels if they were integrated over the distribution of excess shear stress for a given flow [*Gomez and Church*, 1989].

[75] Nor does our analysis consider the short-term variability of the flux–discharge relationship. We relate the available bed load transport record of each site to channel and sediment-supply conditions at the time of field measurement. Hence our analysis examines record-average transport phenomena, but does not consider annual, seasonal or flood event variability. For example, annual hysteresis of bed load transport has been observed at some of the Idaho sites [*Moog and Whiting*, 1998]. Nevertheless, the same computational procedure outlined here could be used to develop shorter-term values of a and b for use in equation (6).

## Appendix A: Bed Load Transport Equations

### A1. *Meyer-Peter and Müller* [1948] (by $d_{50ss}$)

[76] The *Meyer-Peter and Müller* [1948] formula is written as

$$q_b = 8\left[\frac{\mathrm{r}_s}{\mathrm{r}_s - \mathrm{r}}\right]\sqrt{\frac{g}{\mathrm{r}}}\left[\left(\frac{n'}{n_t}\right)^{3/2}\mathrm{r}SD - 0.047(\mathrm{r}_s - \mathrm{r})d_{50ss}\right]^{3/2} \quad \text{(A1)}$$

where $q_b$ is the total specific bed load transport rate (dry mass per unit width and time), r and $\mathrm{r}_s$ are water and sediment densities, respectively (assumed equal to 1000 and 2650 kg m$^{-3}$ throughout), $n'/n_t$ is the ratio of particle roughness to total roughness which corrects the total boundary shear stress to the skin friction stress (that portion applied to the bed and responsible for sediment transport), $S$ is channel slope, $D$ is average flow depth, 0.047 is the critical Shields stress, $g$ denotes gravitational acceleration, and $d_{50ss}$ is the subsurface particle size for which 50% of the sediment sample is finer. The original *Meyer-Peter and Müller* [1948] equation specifies the characteristic grain size as the mean particle size of the unworked laboratory sediment mixture, which is reasonably approximated by $d_{50ss}$.

[77] The total roughness ($n_t$) is determined from the *Manning* [1891] equation as

$$n_t = \frac{S^{1/2}R^{2/3}}{V} \quad \text{(A2)}$$

where $V$ is average velocity and $R$ is hydraulic radius. The grain roughness ($n'$) is determined from the *Strickler* [1923] equation as

$$n' = \frac{d_{90s}^{1/6}}{26} \quad \text{(A3)}$$

where $d_{90s}$ is the surface particle size for which 90% of the sediment sample is finer.

### A2. *Meyer-Peter and Müller* [1948] (by $\mathrm{d_i}$)

[78] Here, we modify the *Meyer-Peter and Müller* [1948] formula for transport by size class

$$q_{bi} = 8f_i\left[\frac{\mathrm{r}_s}{\mathrm{r}_s - \mathrm{r}}\right]\sqrt{\frac{g}{\mathrm{r}}}\left[\left(\frac{n'}{n_t}\right)^{3/2}\mathrm{r}SD - \mathrm{t}^*_{ci}(\mathrm{r}_s - \mathrm{r})d_i\right]^{3/2} \quad \text{(A4)}$$

where $q_{bi}$ is the size-specific bed load transport rate, $f_i$ is the proportion of subsurface material in the $i$th size class, $\mathrm{t}^*_{ci}$ is the size-specific critical Shields stress, and $d_i$ denotes mean particle diameter for the $i$th size class. $\mathrm{t}^*_{ci}$ is determined from the *Andrews* [1983] hiding function as

$$\mathrm{t}^*_{ci} = 0.0834(d_i/d_{50ss})^{-0.872} \quad \text{(A5)}$$

We choose the *Andrews* [1983] function because it was derived from channel types and physiographic environments similar to those examined in this study.

### A3. *Ackers and White* [1973] (by $d_i$)

[79] The *Ackers and White* [1973] equation as modified by *Day* [1980] for size-specific transport is

$$q_{bi} = G_{gri} f_i \mathrm{r}_s d_i V \left(\frac{V}{u^*}\right)^n \tag{A6}$$

where $u^*$ denotes shear velocity

$$u^* = \sqrt{gDS} \tag{A7}$$

and $G_{gri}$ is the dimensionless transport rate of the $i$th size class, defined as

$$G_{gri} = C\left[\frac{F_{gri}}{A_i} - 1\right]^m \tag{A8}$$

[80] $F_{gri}$ is the dimensionless particle mobility parameter (analogous to a noncritical Shields stress), $A_i$ is a dimensionless hiding function analogous to a critical Shields stress, and $C$ and $m$ are empirical values. $F_{gri}$ is defined as

$$F_{gri} = \frac{u^{*n}}{\left(gD\frac{\mathrm{r}_s - \mathrm{r}}{\mathrm{r}}\right)^{\frac{1}{2}}}\left[\frac{V}{\sqrt{32}\log\left(\frac{10D}{d_i}\right)}\right]^{1-n} \tag{A9}$$

where $n$ is an empirical parameter that accounts for mobility differences between the fine and coarse components of the bed load [*Ackers and White*, 1973]. $A_i$, $C$, $m$, and $n$ are functions of dimensionless particle size ($D_{gri}$)

$$D_{gri} = d_i\left[g(\mathrm{r}_s - \mathrm{r})/\left(\mathrm{r}\nu^2\right)\right]^{1/3} \tag{A10}$$

where $\nu$ denotes kinematic viscosity (water temperature assumed 15 C throughout).

[81] For $1 < D_{gri} \leq 60$

$$n = 1 - 0.56\log\left(D_{gri}\right) \tag{A11}$$

$$m = \frac{9.66}{D_{gri}} + 1.34 \tag{A12}$$

$$C = 10^{\left[2.86\log\left(D_{gri}\right) - \left(\log\left(D_{gri}\right)\right)^2 - 3.53\right]} \tag{A13}$$

$$A_i = \left[0.4\left(\frac{d_i}{D_A}\right)^{-1/2} + 0.6\right]A \tag{A14}$$

where

$$D_A = d_{50ss}\left[1.62\sqrt{\frac{d_{84ss}}{d_{16ss}}}^{-0.55}\right] \tag{A15}$$

$$A = \left(\frac{0.23}{\sqrt{D_{gri}}}\right) + 0.14 \tag{A16}$$

and $d_{84ss}$ and $d_{16ss}$ are, respectively, the subsurface particle sizes for which 84% and 16% of the sediment sample is finer. *Day* [1980] defines equation (A15) in terms of grain size percentiles of the unworked laboratory sediment mixture, which we approximate here by the subsurface grain size distribution.

[82] For $D_{gri} > 60$

$$n = 0 \tag{A17}$$

$$m = 1.5 \tag{A18}$$

$$C = 0.025 \tag{A19}$$

$$A_i = \left[0.4\left(\frac{d_i}{D_A}\right)^{-1/2} + 0.6\right]A \tag{A20}$$

where

$$A = 0.17 \tag{A21}$$

### A4. *Bagnold* [1980] (by $d_{mqb}$)

[83] The *Bagnold* [1980] formula is

$$q_b = \left[\frac{\mathrm{r}_s}{\mathrm{r}_s - \mathrm{r}}\right]q_{b*}\left[\frac{\mathrm{w} - \mathrm{w}_0}{(\mathrm{w} - \mathrm{w}_0)_*}\right]^{3/2}\left(\frac{D}{D_*}\right)^{-2/3}\left(\frac{d_{mqb}}{d_*}\right)^{-1/2} \tag{A22}$$

where $q_{b*}$ denotes the reference transport rate (0.1 kg s$^{-1}$ m$^{-1}$), w and $\mathrm{w}_0$ are the applied and critical values of unit stream power, respectively, $(\mathrm{w} - \mathrm{w}_0)_*$ denotes the reference excess stream power (0.5 kg s$^{-1}$ m$^{-1}$), $D_*$ is a reference stream depth (0.1 m), $d_*$ denotes the reference particle size (0.0011 m), and $d_{mqb}$ is the modal grain size of a given bed load transport observation.

[84] Unit stream power is defined as

$$\mathrm{w} = \mathrm{r}DSV \tag{A23}$$

Note that this definition of stream power lacks a gravity term, which *Bagnold* [1980] factors out of all of his equations.

[85] Critical unit stream power for unimodal sediments is defined as

$$\mathrm{w}_0 = 5.75\left[\left(\frac{\mathrm{r}_s}{\mathrm{r}} - 1\right)\mathrm{r}0.04\right]^{3/2}\left(\frac{g}{\mathrm{r}}\right)^{1/2} d_{mss}^{3/2}\log\left(\frac{12D}{d_{mqb}}\right) \tag{A24}$$

For bimodal sediments, *Bagnold* [1980] replaces $\mathrm{w}_0$ with $\mathrm{v}_0$, the geometric mean of the critical stream power for the two modes

$$\mathrm{v}_0 = \left[(\mathrm{w}_0)_1(\mathrm{w}_0)_2\right]^{1/2} \tag{A25}$$

where $(\mathrm{w}_0)_1$ and $(\mathrm{w}_0)_2$ are solved individually from (A24), but with $d_{mqb}$ replaced by the modes of the bed load size distribution ($d_{m1}$ and $d_{m2}$, respectively). Separate computations of (A22) were made under bimodal conditions, replacing $d_{mqb}$ with $d_{m1}$ for one set of computations and $d_{m2}$ for the second set of computations [*Bagnold*, 1980],

which were then summed to determine the total bed load transport of each event.

### A5. *Bagnold* [1980] (by $d_{mss}$)

[86] We use the same approach as above, but with the modal grain size defined from the subsurface material ($d_{mss}$) (a proxy for the high-flow bed load distribution).

### A6. *Parker et al.* [1982] (by $d_{50ss}$)

[87] The *Parker et al.* [1982] formula is

$$q_b = \sqrt{g}(DS)^{3/2} G(\mathrm{f}_{50ss}) W_r^* \frac{\mathrm{r}_s}{\mathcal{R}} \tag{A26}$$

where $W_r^*$ is the reference dimensionless transport rate (equal to 0.0025), $\mathcal{R}$ is the submerged specific gravity of sediment ($\mathrm{r}_s/\mathrm{r} - 1$), and $G(\mathrm{f}_{50ss})$ is a three-part bed load transport function [as revised by *Parker*, 1990] that depends on the excess Shields stress of the median subsurface grain size ($\mathrm{f}_{50ss}$)

$$G(\mathrm{f}_{50ss}) = 5474\left(1 - \frac{0.853}{\mathrm{f}_{50ss}}\right)^{4.5} \qquad \mathrm{f}_{50ss} > 1.59 \tag{A27a}$$

$$G(\mathrm{f}_{50ss}) = \exp\left[14.2(\mathrm{f}_{50ss} - 1) - 9.28(\mathrm{f}_{50ss} - 1)^2\right] \qquad 1 \le \mathrm{f}_{50ss} \le 1.59 \tag{A27b}$$

$$G(\mathrm{f}_{50ss}) = \mathrm{f}_{50ss}^{14.2} \qquad \mathrm{f}_{50ss} \le 1 \tag{A27c}$$

[88] The excess Shields stress is defined as the ratio of the applied Shields stress ($\mathrm{t}_{50ss}^*$) to that of the reference value ($\mathrm{t}_{50r}^*$, that capable of producing the reference dimensionless transport rate, $W_r^* = 0.0025$)

$$\mathrm{f}_{50ss} = \left(\frac{\mathrm{t}_{50ss}^*}{\mathrm{t}_{50r}^*}\right) \tag{A28}$$

[89] The applied Shields stress is given by

$$\mathrm{t}_{50ss}^* = \frac{\mathrm{t}_0}{\mathrm{rg}\ \mathcal{R}\ d_{50ss}} \tag{A29}$$

where $\mathrm{t}_0$ is the total boundary shear stress calculated from the depth-slope product (rg*RS*). The reference Shields stress ($\mathrm{t}_{50r}^*$) is empirically determined from site-specific bed load transport data following the procedure described by *Parker et al.* [1982]. Their approach involves regressing size-specific dimensionless transport rates ($W_i^*$)

$$W_i^* = \frac{\mathcal{R}\ \mathrm{q}_{\mathrm{bi}}}{f_i\sqrt{g}(DS)^{3/2}} \tag{A30}$$

against corresponding Shields stress values ($\mathrm{t}_i^*$)

$$\mathrm{t}_i^* = \frac{\mathrm{t}_0}{\mathrm{rg}\ \mathcal{R}\ d_i} \tag{A31}$$

and collapsing the size-specific curves into a single function

$$W_i^* = \mathrm{a}_i \mathrm{t}_i^{*M} \tag{A32}$$

where $M$ is the weighted mean exponent of the size-specific functions of $W_i^*$ versus $\mathrm{t}_i^*$, and $\mathrm{a}_i$ is the size-specific coefficient of regression [*Parker et al.*, 1982]. Finally, $\mathrm{t}_{50r}^*$ is determined from equation (A32) for the reference transport rate ($W_i^* = W_r^* = 0.0025$) and the site-specific value of $\mathrm{a}_{50}$.

### A7. *Parker et al.* [1982] (by $d_i$)

[90] The *Parker et al.* [1982] equation by size class ($d_i$) is

$$q_{bi} = f_i\sqrt{g}(DS)^{3/2} G(\mathrm{f}_i) W_r^* \frac{\mathrm{r}_s}{\mathcal{R}} \tag{A33}$$

where $\mathrm{f}_i$ denotes the size-specific excess Shields stress

$$\mathrm{f}_i = \left(\frac{\mathrm{t}_i^*}{\mathrm{t}_{ri}^*}\right) \tag{A34}$$

which replaces $\mathrm{f}_{50ss}$ in equation (A27) for solution of $G(\mathrm{f}_i)$. $\mathrm{t}_{ri}^*$ values are determined from site-specific bed load transport data as described above for *Parker et al.* [1982] by $d_{50ss}$.

### A8. *Parker et al.* [1982] (by $d_i$ via *Andrews* [1983])

[91] Here we use the same approach as above, but $\mathrm{t}_{ri}^*$ values are determined from the *Andrews* [1983] hiding function (A5).

[92] **Acknowledgments.** This research was partially funded by the USDA Forest Service, Yankee Fork Ranger District (00-PA-11041303-071). We are grateful for the generous assistance of Sandra Ryan in providing many of the test site data sets. We appreciate the insightful reviews provided by Bill Emmett, Peter Goodwin, David Turner and two anonymous reviewers.

## References

Ackers, P., and W. R. White (1973), Sediment transport: New approach and analysis, *J. Hydraul. Div. Am. Soc. Civ. Eng.*, *99*, 2041–2060.

Almedeij, J. H., and P. Diplas (2003), Bedload transport in gravel-bed streams with unimodal sediment, *J. Hydraul. Eng.*, *129*, 896–904.

Andrews, E. D. (1983), Entrainment of gravel from naturally sorted riverbed material, *Geol. Soc. Am. Bull.*, *94*, 1225–1231.

Andrews, E. D., and J. M. Nankervis (1995), Effective discharge and the design of channel maintenance flows for gravel-bed rivers, in *Natural and Anthropogenic Influences in Fluvial Geomorphology*, *Geophys. Monogr. Ser.*, vol. 89, edited by J. E. Costa et al., pp. 151–164, AGU, Washington, D. C.

Bagnold, R. A. (1980), An empirical correlation of bedload transport rates in flumes and natural rivers, *Proc. R. Soc. London*, *372*, 453–473.

Barnes, H. H. (1967), Roughness characteristics of natural channels, *U.S. Geol. Surv. Water Supply Pap.*, *1849*, 213 pp.

Bravo-Espinosa, M., W. R. Osterkamp, and V. L. Lopes (2003), Bedload transport in alluvial channels, *J. Hydraul. Eng.*, *129*, 783–795.

Brown, C. B. (1950), Sediment transportation, in *Engineering Hydraulics*, edited by H. Rouse, pp. 769–857, John Wiley, Hoboken, N. J.

Buffington, J. M., and D. R. Montgomery (1997), A systematic analysis of eight decades of incipient motion studies, with special reference to gravel-bedded rivers, *Water Resour. Res.*, *33*, 1993–2029.

Buffington, J. M., and D. R. Montgomery (1999a), Effects of hydraulic roughness on surface textures of gravel-bed rivers, *Water Resour. Res.*, *35*, 3507–3522.

Buffington, J. M., and D. R. Montgomery (1999b), Effects of sediment supply on surface textures of gravel-bed rivers, *Water Resour. Res.*, *35*, 3523–3530.

Bunte, K., S. R. Abt, J. P. Potyondy, and S. R. Ryan (2004), Measurement of coarse gravel and cobble transport using portable bedload traps, *J. Hydraul. Eng.*, *130*, 879–893.

Carling, P. (1988), The concept of dominant discharge applied to two gravel-bed streams in relation to channel stability thresholds, *Earth Surf. Processes Landforms*, *13*, 355–367.

Church, M. A., D. G. McLean, and J. F. Wolcott (1987), River bed gravels: Sampling and analysis, in *Sediment Transport in Gravel-Bed Rivers*, edited by C. R. Thorne, J. C. Bathurst, and R. D. Hey, pp. 43–88, John Wiley, Hoboken, N. J.

Cook, R. D., and S. Weisberg (1999), *Applied Regression Including Computing and Graphics*, 590 pp., John Wiley, Hoboken, N. J.

Cui, Y., and G. Parker (2004), Numerical model of sediment pulses and sediment supply disturbances in mountain rivers, *J. Hydraul. Eng*, in press.

Day, T. J. (1980), A study of the transport of graded sediments, *Rep. IT 190*, 10 pp., Hydraul. Res. Stn. Wallingford, U. K.

Dietrich, W. E., J. Kirchner, H. Ikeda, and F. Iseya (1989), Sediment supply and the development of the coarse surface layer in gravel-bedded rivers, *Nature*, *340*, 215–217.

Edwards, T. K., and G. D. Glysson (1999), Field methods for measurement of fluvial sediment, *U.S. Geol. Surv. Tech. Water Resour. Book 3*, Chap. 2, 89 pp.

Einstein, H. A. (1950), The bed-load function for sediment transportation in open channel flows, *Tech. Bull. 1026*, 73 pp., *Soil Conserv. Serv.*, Washington, D. C.

Emmett, W. W. (1980), A field calibration of the sediment-trapping characteristics of the Helley-Smith bedload sampler, *U.S. Geol. Surv. Prof. Pap.*, *1139*, 44 pp.

Emmett, W. W., and M. G. Wolman (2001), Effective discharge and gravel-bed rivers, *Earth Surf. Processes Landforms*, *26*, 1369–1380.

Fang, D. (1998), Book review of: *Sediment Transport Theory and Practice* by C. T. Yang, *Int. J. Sed. Res.*, *13*, 74–83.

Ferguson, R. I. (2003), The missing dimension: Effects of lateral variation on 1-D calculations of fluvial bedload transport, *Geomorphology*, *56*, 1–14.

Ferguson, R. I., T. B. Hoey, S. J. Wathen, A. Werritty, R. I. Hardwick, and G. H. Sambrook Smith (1998), Downstream fining of river gravels: Integrated field, laboratory and modeling study, in *Gravel-Bed Rivers in the Environment*, edited by P. C. Klingeman et al., pp. 85–114, Water Resour. Publ., Highlands Ranch, Colo.

Freese, F. (1960), Testing accuracy, *For. Sci.*, *6*, 139–145.

Gomez, B., and M. Church (1989), An assessment of bedload sediment transport formulae for gravel bed rivers, *Water Resour. Res.*, *25*, 1161–1186.

Gordon, N. (1995), Summary of technical testimony in the Colorado Water Division 1 Trial, *U.S. For. Serv. Gen. Tech. Rep. RM, RMRS-GTR-270*, 140 pp.

Helley, E. J., and W. Smith (1971), Development and calibration of a pressure-difference bedload sampler, open file report, 18 pp., U.S. Geological Survey, Reston, Va.

Jackson, W. L., and R. L. Beschta (1982), A model of two-phase bedload transport in an Oregon coast range stream, *Earth Surf. Processes Landforms*, *7*, 517–527.

Kinerson, D. (1990), Bed surface response to sediment supply, M.S. thesis, 420 pp., Univ. of Calif., Berkeley.

King, J. G., W. W. Emmett, P. J. Whiting, R. P. Kenworthy, and J. J. Barry (2004), Sediment transport data and related information for selected gravel-bed streams and rivers in Idaho, *U.S. For. Serv. Gen. Tech. Rep. RM*, *RMRS-GTR-131*, 26 pp.

Laronne, J. B., and I. Reid (1993), Very high rates of bedload sediment transport by ephemeral desert rivers, *Nature*, *366*, 148–150.

Laronne, J. B., C. Garcia, and I. Reid (2000), Mobility of patch sediment in gravel bed streams: Patch character and its implications for bedload, in *Gravel-Bed Rivers V*, edited by M. P. Mosley, pp. 249–280, N. Z. Hydrol. Soc., Wellington.

Leopold, L. B., and W. W. Emmett (1997), Bedload and river hydraulics—Inferences from the East Fork River, Wyoming, *U.S. Geol. Surv. Prof. Pap.*, *1583*, 52 pp.

Leopold, L. B., M. G. Wolman, and J. P. Miller (1964), *Fluvial Processes in Geomorphology*, 552 pp., W. H. Freeman, New York.

Lisle, T. E., and S. Hilton (1999), Fine bed material in pools of natural gravel bed channels, *Water Resour. Res.*, *35*, 1291–1304.

Lisle, T. E., J. M. Nelson, J. Pitlick, M. A. Madej, and B. L. Barkett (2000), Variability of bed mobility in natural, gravel-bed channels and adjustments to sediment load at local and reach scales, *Water Resour. Res.*, *36*, 3743–3755.

Manning, R. (1891), On the flow of water in open channels and pipes, *Trans. Inst. Civ. Eng. Ireland*, *20*, 161–207.

Martin, Y. (2003), Evaluation of bed load transport formulae using field evidence from the Vedder River, British Columbia, *Geomorphology*, *53*, 73–95.

Meyer-Peter, E., and R. Müller (1948), Formulas for bed-load transport, in *Proceedings of the 2nd Meeting of the International Association for Hydraulic Structures Research*, pp. 39–64, Int. Assoc. Hydraul. Res., Delft, Netherlands.

Milhous, R. T. (1973), Sediment transport in a gravel-bottomed stream, Ph.D. dissertation, 232 pp., Oreg. State Univ., Corvallis.

Montgomery, D. R., and J. M. Buffington (1997), Channel-reach morphology in mountain drainage basins, *Geol. Soc. Am. Bull.*, *109*, 596–611.

Moog, D. B., and P. J. Whiting (1998), Annual hysteresis in bed load rating curves, *Water Resour. Res.*, *34*, 2393–2399.

Neter, J., W. Wasserman, and M. H. Kutner (1974), *Applied Linear Statistical Models*, 1181 pp., R. D. Irwin, Inc., Burr Ridge, Ill.

Paola, C., and R. Seal (1995), Grain size patchiness as a cause of selective deposition and downstream fining, *Water Resour. Res.*, *31*, 1395–1407.

Parker, G. (1978), Self-formed straight rivers with equilibrium banks and mobile bed. Part 2. The gravel river, *J. Fluid Mech.*, *89*, 127–146.

Parker, G. (1979), Hydraulic geometry of active gravel rivers, *J. Hydraul. Div. Am. Soc. Civ. Eng.*, *105*, 1185–1201.

Parker, G. (1990), Surface-based bedload transport relation for gravel rivers, *J. Hydraul. Res.*, *28*, 417–436.

Parker, G., and Y. Cui (1998), The arrested gravel front: Stable gravel-sand transitions in rivers, part 1: Simplified analytical solution, *J. Hydraul. Res.*, *36*, 75–100.

Parker, G., and P. C. Klingeman (1982), On why gravel bed streams are paved, *Water Resour. Res.*, *18*, 1409–1423.

Parker, G., P. C. Klingeman, and D. G. McLean (1982), Bedload and size distribution in paved gravel-bed streams, *J. Hydraul. Div. Am. Soc. Civ. Eng.*, *108*, 544–571.

Parker, G., C. M. Toro-Escobar, M. Ramey, and S. Beck (2003), Effect of floodwater extraction on mountain stream morphology, *J. Hydraul. Eng.*, *129*, 885–895.

Pitlick, J. (1994), Relation between peak flows, precipitation, and physiography for five mountainous regions in the western USA, *J. Hydrol.*, *158*, 214–219.

Reid, I., D. M. Powell, and J. B. Laronne (1996), Prediction of bed-load transport by desert flash floods, *J. Hydraul. Eng.*, *122*, 170–173.

Reynolds, M. R. (1984), Estimating error in model prediction, *For. Sci.*, *30*, 454–469.

Ryan, S. E., and W. W. Emmett (2002), The nature of flow and sediment movement in Little Granite Creek near Bondurant, Wyoming, *U.S. For. Serv. Gen. Tech. Rep. RM, RMRS-GTR-90*, 46 pp.

Ryan, S. E., L. S. Porth, and C. A. Troendle (2002), Defining phases of bedload transport using piecewise regression, *Earth Surf. Processes Landforms*, *27*, 971–990.

Sambrook Smith, G. H., and R. I. Ferguson (1995), The gravel-sand transition along river channels, *J. Sed. Res., Sect. A*, *65*, 423–430.

Schoklitsch, A. (1950), *Handbuch des wasserbaues*, Springer-Verlag, New York.

Smith, T. R., and F. P. Bretherton (1972), Stability and the conservation of mass in drainage basin evolution, *Water Resour. Res.*, *8*, 1506–1528.

Strickler, A. (1923), Beitrage zur Frage der Geschwindigheistformel und der Rauhigkeitszahlen für Strome, Kanale und Geschlossene Leitungen, *Mitt. Eidg. Amtes Wasserwirt. 16*, Eidg. Amtes Wasserwirt., Bern.

Swanston, D. N. (1991), Natural processes, in *Influences of Forest and Rangeland Management on Salmonid Fishes and Their Habitat*, *Spec. Publ. 19*, edited by W. R. Meehan, pp. 139–179, Am. Fish. Soc., Bethesda, Md.

U.S. Water Resources Council (1981), Guidelines for determining flood flow frequency, *Bull. 17B*, U.S. Geol. Surv., Reston, Va.

Vanoni, V. A. (1975), Sediment discharge formulas, in *Sedimentation Engineering*, edited by V. A. Vanoni, pp. 190–229, Am. Soc. Civ. Eng., Reston, Va.

Whiting, P. J. (2002), Streamflow necessary for environmental maintenance, *Annu. Rev. Earth Planet. Sci.*, *30*, 181–200.

Whiting, P. J., and J. G. King (2003), Surface particle sizes on armoured gravel streambeds: Effects of supply and hydraulics, *Earth Surf. Processes Landforms*, *28*, 1459–1471.

Whiting, P. J., J. F. Stamm, D. B. Moog, and R. L. Orndorff (1999), Sediment-transporting flows in headwater streams, *Geol. Soc. Am. Bull.*, *111*, 450–466.

Wilcock, P. R. (2001), Toward a practical method for estimating sediment-transport rates in gravel-bed rivers, *Earth Surf. Processes Landforms*, *27*, 1395–1408.

Williams, G. P., B. Thomas, and R. Daddow (1988), Methods for collection and analysis of fluvial-sediment data, *U.S. For. Serv. Tech. Pap. WS, WSDG-TP-00012*, 85 pp.

Wolman, M. G. (1954), Method of sampling coarse river bed material, *Eos Trans. AGU*, *35*, 951–956.

Wolman, M. G., and J. P. Miller (1960), Magnitude and frequency of forces in geomorphic processes, *J. Geol.*, *68*, 54–74.

Yang, C. T., and C. Huang (2001), Applicability of sediment transport formulas, *Int. J. Sed. Res.*, *16*, 335–353.

Zar, J. H. (1974), *Biostatistical Analysis*, 718 pp., Prentice-Hall, Old Tappan, N. J.

J. J. Barry, Boise Cascade Corporation, Timberland Resources, 1111 West Jefferson Street, Boise, ID 83728, USA. (jeffbarry@bc.com)

J. M. Buffington and J. G. King, Rocky Mountain Research Station, USDA Forest Service, Boise, ID 83702, USA.